Canadian Institute of Actuaries | Institut canadien des actuaires

Research paper

Pandemic Risk Management: Resources Contingency Planning and Allocation

Xiaowei Chen, Wing Fung Chong,
Runhuan Feng, Linfeng Zhang
University of Illinois

August 2021

Document rp221089

Ce document est disponible en français

Abstract

The repeated history of pandemics, such as SARS, H1N1, Ebola, Zika, and COVID-19, has shown that pandemic risk is inevitable. Extraordinary shortages of medical resources have been observed in many parts of the world. Some attributing factors include the lack of sufficient stockpiles and the lack of coordinated efforts to deploy existing resources to the locations of greatest need.

This paper investigates contingency planning and resources allocation from a risk management perspective, as opposed to the prevailing supply chain perspective. The key idea is that the competition for limited critical resources is not only present in different geographical locations but also at different stages of a pandemic. This paper draws on an analogy between risk aggregation and capital allocation in finance and pandemic resources planning and allocation for healthcare systems. The main contribution is to introduce new strategies for optimal stockpiling and allocation balancing spatio-temporal competition for medical supply and demand.

1. Introduction

1.1 Lessons From Recent Pandemics

An epidemic is an outbreak of a disease that spreads rapidly to a cohort of individuals in a wide area. According to the definition from the US Centers for Disease Control and Prevention (2012), "pandemic refers to an epidemic that has spread over several countries or continents, usually affecting a large number of people." Because humans have little immunity to the new disease, a pandemic can emerge quickly around the world. One of the most disastrous pandemics in the recent history is the 1918 flu pandemic, which infected around 500 million people and resulted in the deaths of an estimated 50 million worldwide, more than those who died from World War I. Most recently, the novel coronavirus disease of 2019 (COVID-19) is an infectious disease caused by a new virus that only emerged in late 2019 and has since spread to nearly every country in the world. As estimated by the International Monetary Fund (2021), the global economy contracted by 3.5% in 2020. However, COVID-19's far-reaching impact and the consequent economic fallout due to the loss of productivity are yet to be realized; as of May 8, 2021, the number of infected cases had accumulated to over 157 million worldwide, with the death toll reaching over 3.2 million (see, for example, Worldometer, 2021).

The repeated history of pandemics in recent decades, such as SARS, swine flu, Ebola, and the most recent, COVID-19, has taught us that pandemic risk is inevitable. Recent research studies (see, for instance, Morse, 1995; Jones et al., 2008) have shown that the frequency of pandemics has increased over the past century due to increased social connectivity, long-distance travel, urbanization, changes in land use, trade, consumption of wild animals, and greater exploitation of the natural environment. Based on the data collected from various sources (for example, Centers for Disease Control and Prevention, 2018; World Health Organization, 2018; World Health Organization, 2019), Figure 1 is created to visualize both the frequency and severity of well-recognized pandemics and public health emergencies of international concern declared by the WHO since the 1900s. The vertical axis represents the number of documented infections on a logarithmic scale. Both the size and color scale of the circles indicate the number of deaths resulting from the pandemics and public health emergencies. The alarming pattern of increased frequency clearly points to the critical importance of pandemic risk management.

Figure 1: Frequency and severity of pandemics and public health emergencies since the 1900s

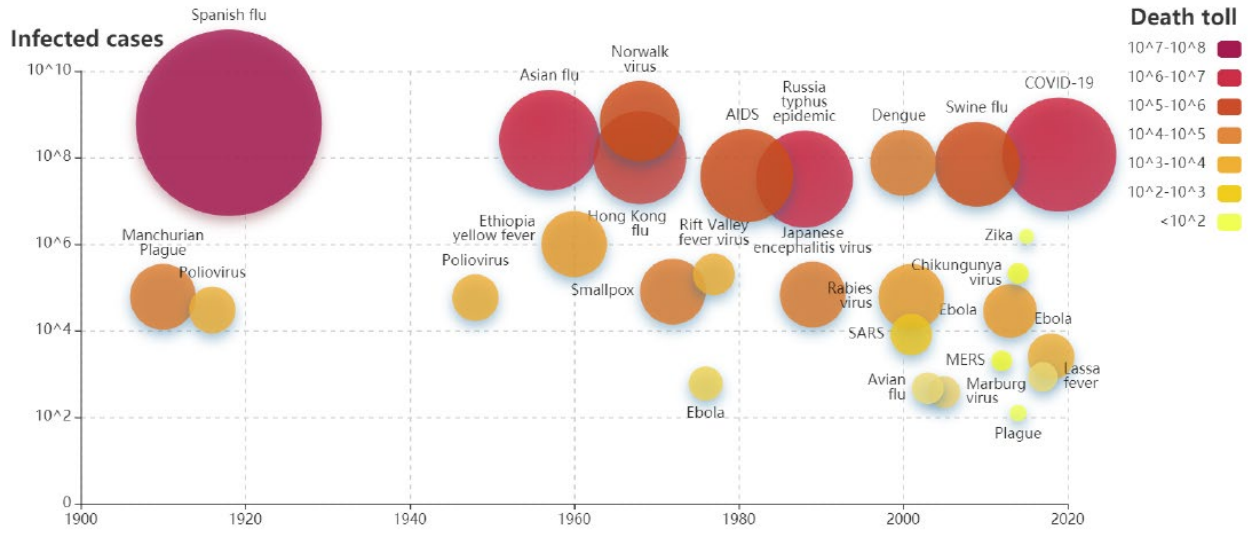

Governments around the world have been taking the blame for their failure to promptly implement appropriate policies to contain the pandemic. Many countries experienced severe shortages of resources. Ranney, Griffeth, and Jha (2020) studied the critical role of scarce resources, such as ventilators and personal protective equipment (PPE), in shaping the direction of COVID-19. Such an unprecedented challenge exposes the inadequacy of contingency planning and resources-allocation strategies of public health systems. The lack of planning drove policymakers to make impromptu decisions on resources acquisition and allocations that may have exacerbated the extraordinary shortage.

The United States boasts one of the best healthcare systems, with a large network of healthcare professionals, the best-equipped medical facilities and hospitals, and the most advanced medical technology. Yet, the country was underprepared for the COVID-19 pandemic. There were severe shortages of diagnostic and preventative medical supplies both for healthcare providers and the general public in many states in the early stage of the pandemic, which made it difficult for public authorities to contain it. According to a recent report by President Obama's former advisors on science and technology (Holdren et al., 2020), there were several contributing factors to the lack of medical resources:

1. *National reserves of critical medical supplies were not replenished sufficiently prior to COVID-19*. The Strategic National Stockpile (SNS) was established by the US government in 2003 as the national repository of pharmaceutical and vaccination stockpiles. The SNS relies on the appropriation of funding from Congress. Much of the mask stockpile was depleted during the 2009 H1N1 pandemic, and Congress did not act quickly enough to provide the funding to replenish the stockpile to the appropriate level projected by many studies.
2. *In order to minimize inventory cost and improve efficiency, many manufacturers and supply chain managers of medical supplies shifted to just-in-time (JIT) inventory systems prior to the pandemic. Goods were received only just in time for production and distribution*. The JIT system relies on the ability of manufacturers to accurately predict

demand. The initial public policies such as lockdowns caused major disruptions to supply chains around the world, and there were insufficient inventories to absorb surging demand.

3. *There was a lack of sufficient coordination among federal and state governments to deploy existing resources to the most devastated areas in the country*. Healthcare professionals are put at high risk when treating patients without sufficient PPE. It was difficult to uncover and contain the spread of disease without adequate testing. Several states in the United States acted on their own to secure supplies from foreign manufacturers, and engaged in a bidding war for limited supplies (Estes, 2020). Existing resources were not necessarily distributed on a basis of health need (Tobin-Tyler, 2020). Many of the hardest-hit states have had to ration care, while other states have had low utilization of their resources.

While there are policy-related issues that require policymakers' action, academics can contribute to the understanding of pandemic evolution and the resulting dynamics of demand and supply. There is a clear need for the development of a scientific foundation for adaptive strategies for balancing demand and supply and rationing limited resources. Contingency planning and resources allocation in a centralized form have been advocated as two coherent strategies to mitigate catastrophic economic consequences from a pandemic; see, for example, Jamison et al. (2017). Ranney, Griffeth, and Jha (2020) argued that the government should have tracked the use of resources and the projection of needs in all subsidiaries, and should have coordinated allocation of resources to reduce shortages across subsidiaries and over time in the course of a pandemic. A comparable example of centralized planning is the Federal Emergency Management Agency, which administers many pre-disaster risk mitigation programs, such as national flood insurance, mitigation grants, and post-disaster response plans, including search and rescue teams, medical assistance teams and monetary relief; see Vanajakumari, Kumar, and Gupta (2016) and Stauffer and Kumar (2021) for information.

Centralized planning and resources allocation have long been practised as risk management strategies in the financial industry. For example, banks and insurers are heavily regulated by governments to ensure their capabilities to absorb severe financial losses and endure adverse economic scenarios (Segal, 2011). The central hypothesis of this paper is that many risk aggregation and capital allocation techniques drawn from financial and insurance literature can be extended and applied to pandemic resources planning and allocation.

Figure 2: New York, Florida, and California experience different phases of COVID-19, based on data as of September 12, 2020 from *The Atlantic* (2020)

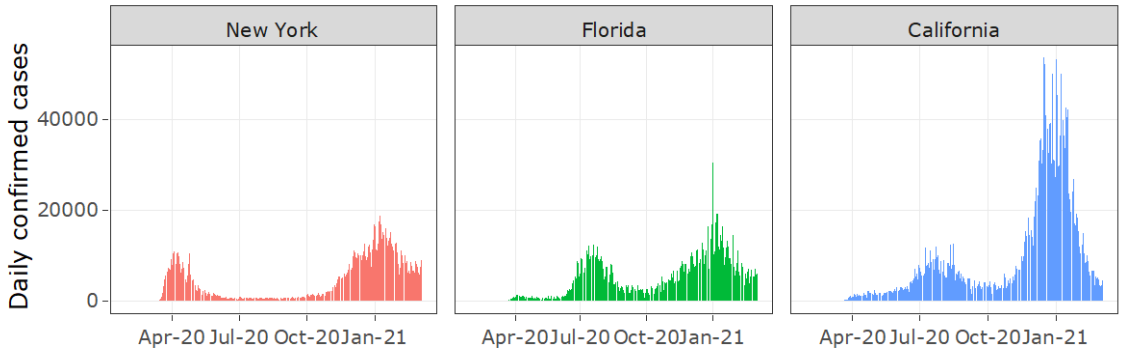

1.2 Case Study

Figure 2 depicts the daily confirmed COVID-19 cases in the states of New York, Florida, and California in 2020 and 2021. More specifically, the timespan of data used in this paper is from March 2020 to March 2021. One could observe that, among these three states, New York was first hit the hardest by the pandemic in April 2020, while both Florida and California experienced the first peak of cases around July and August in that year; moreover, although both New York and Florida showed comparatively fewer cases in January 2021, California was savaged by COVID-19 around that time.

Let us do a thought experiment for the moment. Imagine that these three states established a resource-pooling alliance prior to the pandemic. They could have complemented each other by delivering one state's surplus resources to aid another in deficit. For example, in April 2020 the alliance could have coordinated the efforts to send initial stockpiles and increase emergency production to support New York; by July and August 2020, when both Florida and California were hit the hardest, unused resources in New York could be made available to both Florida and California; in January 2021 the remaining resources, together with additional production, should have been redirected from both New York and Florida to California. Such a coalition is not unimaginable even in a decentralized political system like the United States. In April 2020, six northeastern states (New York, Connecticut, New Jersey, Rhode Island, Pennsylvania, and Delaware) formed a government procurement coalition for critical medical equipment in an effort to avoid a bidding war (Holveck, Racioppi, and Shanes, 2020).

The purpose of this paper is to propose an overarching framework for different regions to optimize stockpiling and resources allocation at different pandemic stages in order to best utilize limited resources. While the alliance of the above three states is used as an illustrative example throughout this paper, the proposed framework can also be implemented in coordination among other administrative divisions, such as provinces and territories in Canada, as well as international collaboration on the production, procurement, distribution, and pooling of resources.

1.3 Pandemic Risk Management Framework and Contribution

A vast amount of recent literature on COVID-19 focuses on the prediction of transmission dynamics (e.g. Fernández-Villaverde and Jones, 2020; Hortaçsu, Liu, and Schwieg, 2021), infected cases (e.g. Giordano et al., 2020), economic impact (e.g. Acemoglu et al., 2020; Gregory, Menzio, and Wiczer, 2020), and the effect of non-pharmaceutical intervention and other public policies (e.g. Charpentier et al., 2020). However, to the best of our knowledge, academic research on quantitative frameworks for contingency planning and resources allocation in response to pandemic risk is rare. While the banking and insurance industries have long had a rich tradition of developing technologies for robust risk management, the focus has been largely on financial and insurable risks. This paper aims to take advantage of the vast medical literature on epidemic modelling and apply classic concepts from risk management and insurance literature, such as reserving and capital allocation, to pandemic risk management.

Strategic pandemic planning requires scientific assessment, rather than on-the-fly ad hoc decisions and patchworks for damage control. In accordance with current practices of national pandemic preparedness and control strategies around the world, we summarize and propose a three-pillar framework for quantitative pandemic risk management:

- *Pillar I: Regional and Aggregate Resources Supply and Demand Forecast*. Any pre-pandemic preparation plan should consist of a supply-and-demand assessment and forecast. The supply side should include inventory assessments of critical resources and supplies, the maximum capacity of services, and the capability of emergency acquisition and production. The demand side requires an understanding of the dynamics of a potential pandemic across regions and across borders. Historical data and predictive models can be used to project the evolution of a pandemic and the resulting surge in demand around a healthcare system.
- *Pillar II: Centralized Stockpiling and Distribution*. A central authority coordinates the efforts to develop a national preparedness strategy and to set up reserves of critical resources, including preventative, diagnostic, and therapeutic resources. A response plan is also necessary to understand how the central authority can deliver resources to different regions quickly to meet surges in demand and to balance competing interests and priorities.
- *Pillar III: Central–Regional Resources Allocation*. A pandemic response plan is critical for a central authority to contain and control the spread of a pandemic in regions under its jurisdiction. As demand may exceed any best-effort pre-pandemic projection, the authority needs to devise optimal strategies that best utilize limited existing resources and minimize the economic cost of supply–demand imbalance. A coordination strategy needs to be in place to ensure smooth communications with regional authorities. The allocation strategy should be based on scientifically sound methods, taking into account spatio-temporal differences across regions to ensure fairness and impartiality.

Figure 3: Three-pillar pandemic risk management framework

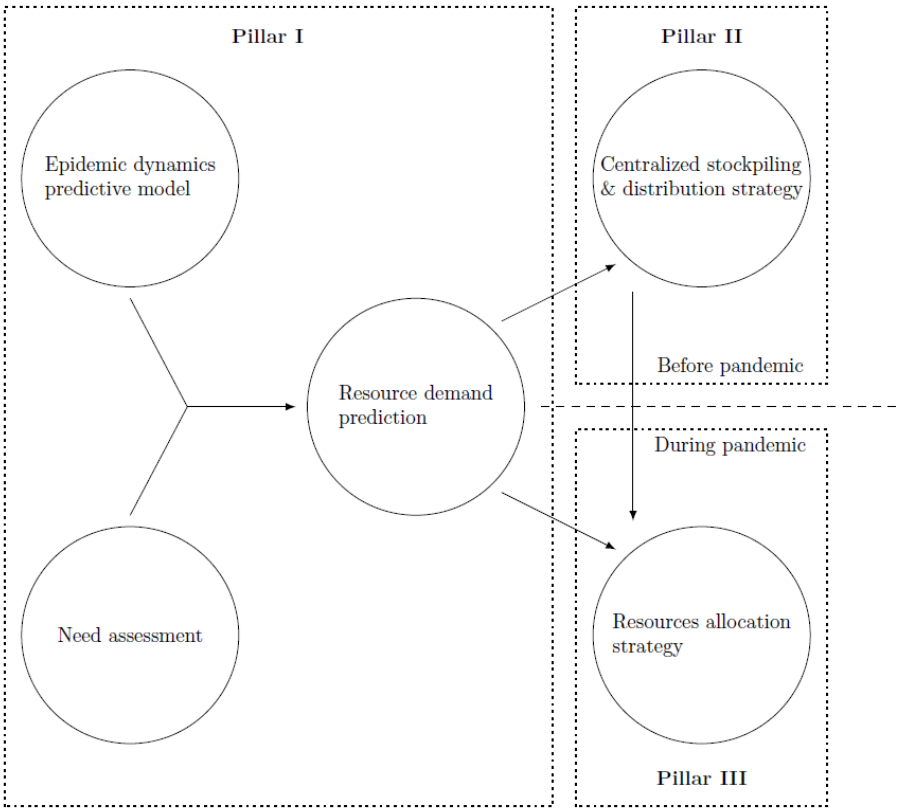

It should be pointed out that while the first pillar is not the focus of this paper, it plays a critical role in ensuring the adequacy and effectiveness of planning and responses in the second and third pillars.

The proposed framework applies regardless of predictive models for projecting reported cases. The main technical contribution of this paper lies in the second and third pillars, for which we propose strategies for centralized resource stockpiling, distribution, and allocation.

Table 1: Comparison between capital and pandemic risk management

Capital risk management	Pandemic risk management
Business line and aggregate risk	Regional and aggregate resources demand
Risk-based capital	Centralized stockpiling
Business line capital allocation	Centralized distribution and allocation
Trade-off between surplus/deficiency and cost of capital	Balance of supply/demand and economic cost

The paper draws inspiration from two sources in insurance and risk management literature:

1. Insurance applications of epidemic models. Early applications of epidemic compartment models appeared in Hua and Cox (2009), in which real option pricing is used for operational risk management, and Feng and Garrido (2011), which analyzed epidemic insurance coverage. The study of epidemic insurance was extensively developed in a stochastic setting in Lefèvre, Picard, and Simon (2017), Lefèvre and Picard (2018), and Lefèvre and Simon (2020), and more recently included in the assessment of cyber risk by Hillairet and Lopez (2021). All of these compartmental models can be used in Pillar I.
2. Capital allocation. The subject of capital management is well studied in the insurance literature. The applications of reserving and capital allocation form the basis of the proposed Pillars II and III. Table 1 reveals how our proposed framework shadows the classical capital risk management. While spatial balancing of allocation is well known in banking and insurance (see, for instance, Dhaene et al., 2012; Chong, Feng, and Jin, 2021), this paper develops a *novel spatio-temporal balancing* of resources distribution and allocation, which, to the best of our knowledge, has not previously been studied in either financial or management literature.

The rest of the paper is organized as follows. Each of the next three sections provides detailed discussion of one of the three pillars in the proposed pandemic risk management framework, as well as economic interpretations of resulting optimal strategies. Numerical examples are embedded in the discussion for better clarity. We conclude in the last section with discussions of potential applications and future work.

2. Pillar I: Regional and Aggregate Resources Demand Forecast

In the pre-pandemic time, a central authority should first model the pandemic transmission dynamics in each region. Regardless of the choice of epidemiological models, that authority should calibrate the model in each region by its preparedness and other contingency measurements. Indeed, epidemic forecast models have been used for healthcare policy making and public communications; see, for example, Leung et al. (2020) and Tian et al. (2020). In this paper, in line with CovidActNow (2020) and Hill et al. (2020), the population in each region is divided into seven mutually exclusive compartments, namely the susceptible (*S*), the exposed (*E*), the mildly infected (I_1), the infected with hospitalization (I_2), the infected with intensive care (I_3), the recovered (*R*), and the deceased (*D*). The dynamics among these seven compartments are governed by a set of ordinary differential equations, and the model is, in short, called the SEIRD.

This SEIRD model is characterized by a set of ordinary differential equations that describe population flows among all the aforementioned compartments:

$$
\begin{aligned}
\mathrm{d}S(t) &= -(\beta_1 I_1(t) + \beta_2 I_2(t) + \beta_3 I_3(t))S(t)\ \mathrm{d}t, \\
\mathrm{d}E(t) &= [(\beta_1 I_1(t) + \beta_2 I_2(t) + \beta_3 I_3(t))S(t) - \gamma E(t)]\ \mathrm{d}t, \\
\mathrm{d}I_1(t) &= [\gamma E(t) - (\delta_1 + p_1)I_1(t)]\ \mathrm{d}t, \\
\mathrm{d}I_2(t) &= [p_1 I_1(t) - (\delta_2 + p_2)I_2(t)]\ \mathrm{d}t, \\
\mathrm{d}I_3(t) &= [p_2 I_2(t) - (\delta_3 + \mu)I_3(t)]\ \mathrm{d}t, \\
\mathrm{d}R(t) &= [\delta_1 I_1(t) + \delta_2 I_2(t) + \delta_3 I_3(t)]\ \mathrm{d}t, \\
\mathrm{d}D(t) &= \mu I_3(t)\ \mathrm{d}t.
\end{aligned}
$$

All parameters in the set of equations bear clinical meanings; $\beta_i,\ i$ = 1, 2, 3 is the transmission rate of the infected class $I_i;\ 1/\gamma$ is the average latency period; $1/\delta_i,\ i$ = 1, 2, 3 is the average duration of infection in the class I_i before recovery to the class $R;\ p_i,\ i$ = 1, 2, 3 represents the rate at which conditions worsen and individuals require healthcare at the next level of severity; μ is the rate for the most severe cases in the class I_3 to move to the deceased class *D*.

Suppose that the total number of individuals in the entire population is *N.* Each of the ordinary differential equations represents a decomposition of instantaneous change in the population of a compartment. For example, the first equation shows that the instantaneous rate of reduction in the number of the susceptible, − d*S*(*t*), matches the sum of the rates of infection due to contacts with the infected of all classes, $\beta_1 I_1(t)S(t) + \beta_2 I_2(t)S(t) + \beta_3 I_3(t)S(t)$. The products are due to the law of mass action in biology. For example, the rate of secondary infection by the mildly infected, $(\beta_1 N) I_1(t)(S(t)/N)$, can be interpreted as the number of adequate contacts each infected makes to transmit the disease $\beta_1 N$ multiplied by the number of infected $I_1(t)$, multiplied by the percentage that each contact is made with a susceptible person, $S(t)/N$. All other equations can be explained in similar ways. The estimations of these model parameters are well studied in the literature for COVID-19 as well as other pandemics; see, for example, Wu and McGoogan (2020), P. Yang et al. (2020), and X. Yang et al. (2020).

Based on these parameters, the basic reproductive ratio R_0 of a pandemic is given by:

$$R_0 = \frac{N}{p_1 + \delta_1}\left(\beta_1 + \frac{p_1}{p_2 + \delta_2}\left(\beta_2 + \beta_3 \frac{p_2}{\mu + \delta_3}\right)\right).$$

The basic reproductive ratio R_0 can be estimated by empirical data and is often used to calibrate other parameters. In what follows, we shall use a discretized version of the compartmental model. For example, we use the notation $I_{1,j} = I_1(j\Delta t)$ to indicate the number of mild cases projected on the j-th period each with the length Δt. We sometimes omit the information on Δt as the time unit may vary depending on the reporting period.

It is worth noting that estimating the parameters in the SEIRD model is not easy in practice. Its estimation accuracy is often limited by the quality of data. For example, the number of positive cases in a region can be altered by its testing capacity, and in turn affects the positivity data quality. However, we emphasize that the SEIRD model is widely accepted and it should be accurate as long as the model parameters are estimated with accurate data input.

Based on predictive models such as the above-mentioned regional SEIRD models, a central authority could predict, prior to a pandemic or at the onset of a pandemic, changes in demand over the course of the pandemic. Resources require different stockpiling and allocation strategies, depending on their shelf lives.

In this paper, we consider two types of medical resources, namely durable and single-use. Durable resources are those that can perform their required functions for a lengthy period of time without significant expenditure on maintenance or repair. Single-use resources are those that are designed to be used once and then disposed of. Mechanical ventilators and PPE are used as representative examples of durable and single-use resources respectively in this paper.

Table 2: Percentage of severe intensive care unit (ICU) infected cases requiring ventilators

	$\alpha \in [0,1]$	Data source
China	$< 20\%$	X. Yang et al. (2020)
Italy	$[87\%, 90\%]$	Grasselli et al. (2020)
Seattle	75%	Bhatraju et al. (2020)
Washington	71.4%	Arentz et al. (2020)

Durable Resources: Ventilators

Based on the findings in the medical literature (references within Table 2), there are estimates of the percentage α of the infected with intensive care that require the use of mechanical ventilators. These regional differences can be addressed in separate regional compartment models.

We can use these estimates to project the ventilator demand by $X_j^{\mathrm{VEN}(i)} = \alpha I_{3,j}^{(i)}$, where i indicates the i-th region in the alliance and j indicates the j-th day of the pandemic. The model can also be extended to include time-varying percentages of severe patients requiring ventilators. The calculations in the rest of the paper would carry through. Figure 4(a) below shows the projected ventilator demands in New York, Florida, and California based on the

SEIRD model proposed by CovidActNow (2020), which is calibrated to publicly available reported cases as of March 5, 2021, and demand assessment parameters in Appendix B.

Single-Use Resources: Personal Protective Equipment

The assessment of need for PPE sets varies by the patients' class and the severity of their medical conditions in care, and the function of medical professionals. Table 3 offers an example of such a need assessment by the European Centre for Disease Prevention and Control (2020). Given these estimates, we can project the regional PPE set demand by $X_j^{\mathrm{PPE}(i)} = \theta^{E}\left(S_{j-1}^{(i)} - S_j^{(i)}\right) + \theta^{I_2} I_{2,j}^{(i)} + \theta^{I_3} I_{3,j}^{(i)}$, where θ^{E} is the number of PPE sets per exposed case, θ^{I_2} is the number of PPE sets per day per hospitalized patient, and θ^{I_3} is the number of PPE sets per day per intensive care patient. Note that $S_{j-1} - S_j$ represents the daily exposed cases whereas $I_{2,j}$ and $I_{3,j}$ keeps track of existing infected cases that require medical attention. Figure 4(b) below shows how ventilator and PPE demands are projected to evolve over time for New York, Florida, and California, based on the model by CovidActNow (2020) and the PPE need assessment in Appendix B.

In the first pillar, the central authority is expected to work with regional authorities and healthcare professionals to predict the dynamics of regional demands. All regional data are then compiled and aggregated to form the basis of forecasts for the system-wide resource demand. Suppose that there are a total of *n* regions in a healthcare system or medical resource alliance. For example, the aggregate ventilator demand can be determined by $X_j^{\mathrm{VEN}} = \sum_{i=1}^{n} X_j^{\mathrm{VEN}(i)}$, while the aggregate PPE set demand may be given by $X_j^{\mathrm{PPE}} = \sum_{i=1}^{n} X_j^{\mathrm{PPE}(i)}$.

Figure 5 below shows how the aggregate ventilator and PPE demand prediction for the COVID-19 pandemic could have been made in the hypothetical example of a three-state resources-pooling alliance.

Table 3: Minimum amount of PPE sets for different scenarios

	Suspected	Infected hospitalized cases	Infected intensive care cases
Healthcare staff	Number of sets per case θ^{E}	Number of sets per day per patient	
		θ^{I_2}	θ^{I_3}
Nursing	1–2	6	6–12
Medical	1	2–3	3–6
Cleaning	1	3	3
Assistant nursing and other services	0–2	3	3
Total	3–6	14–15	15–24

Figure 4: Ventilator and PPE regional demand prediction in New York, Florida, and California alliance

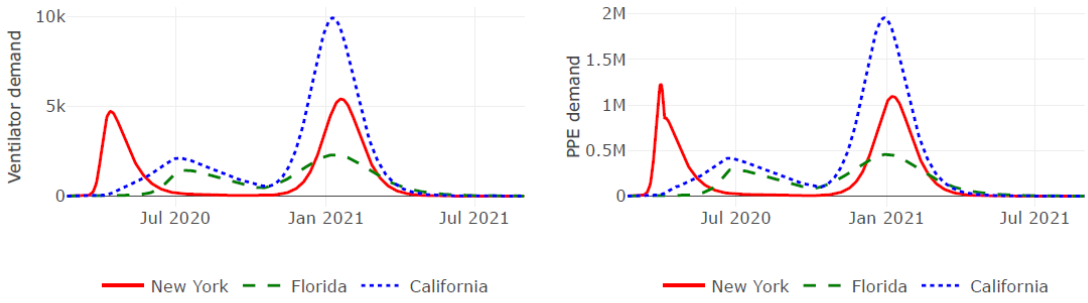

(a) Ventilator (b) Personal protective equipment

Observe that projections for ventilators and PPE sets show very similar patterns as both were driven by the same SEIRD model. The peaks in demand for ventilators are delayed compared with those for PPE sets in Figure 5 due to the fact that it may take a few days before newly diagnosed patients develop symptoms that require ventilator intervention. The projection of regional and aggregate demands offers health authorities a clear understanding of the *temporal competition* of critical resources.

It should be pointed out that predictive models in Pillar I, such as the SEIRD model introduced in this section, are used for multiple purposes, as shown in Figure 3. First, they need to be developed prior to a pandemic using historical data, and to form the basis of demand forecasts for contingency planning in Pillar II. Then, as a pandemic starts to emerge, the predictive models also need to be recalibrated and updated with the latest medical knowledge and reported cases. New forecasts would then be fed into models to determine the optimal allocation strategies in Pillar III. As medical knowledge of the viral disease evolves and predictive models improve over time, Pillars I and III may be revisited from period to period. When a distribution schedule of resources requires an update, we can go back to Pillar II. Therefore, the three-pillar framework may be utilized in circles such as Pillars I, II, III, I, III, I, III, I, II, III, etc. This shall be further elaborated at the end of this paper.

Figure 5: Ventilator and PPE aggregate demand prediction in New York, Florida, and California

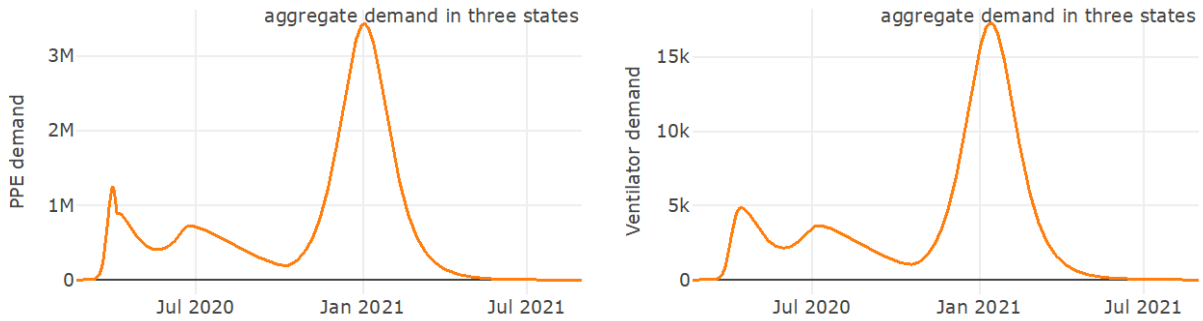

3. Pillar II: Centralized Stockpiling and Distribution

As the pandemic unfolds, many hospitals and healthcare facilities may run out of pharmaceuticals and other essential resources before emergency production can pick up and additional supplies become available. To meet the surge in demand at the onset of a pandemic, many countries maintain national repositories of antibiotics, vaccines, chemical antidotes, antitoxins, and other critical medical supplies. A *centralized stockpiling strategy* is intended to provide a stopgap measure to meet the surge in resources demand at the early stage of the pandemic. There is well-established literature on stockpiling strategies for influenza pandemics; see, for example, Greer and Schanzer (2013) and Siddiqui and Edmunds (2008).

One should keep in mind that a practical stockpiling strategy is often an act of *balance between adequate supply and economic cost*. On one hand, under-stocking is a common issue as resources and their storage can involve heavy costs, and the actual demand during the pandemic outbreak could deviate from the projection; for example, Ellison (2020) claimed that as many as 20 states in the United States were expected to encounter shortages in ICU beds when COVID-19 cases peaked. On the other hand, excessive stockpiling for the long term could lead to unnecessary waste, especially for disposable and perishable resources; for instance, Facher (2020) reported that in March 2020, during the COVID-19 pandemic, the SNS in the United States stocked 13 million N95 masks, of which as many as 5 million may have expired, partly contributing to the nationwide shortage of masks.

In the second pillar of our proposed framework, based on the estimated aggregate resources demand, the central authority could then develop stockpiling and distribution strategies in the time before a pandemic. Notice that durable resources such as ventilators can be reused throughout the pandemic, while single-use resources such as PPE sets must be disposed of after one-time usage. Hence, we have to treat them separately for optimal centralized stockpiling and distribution strategies.

3.1 Durable Resources: Ventilators

It is typical that a central authority has to determine an optimal initial stockpile size K_0 of resources to maintain in some centralized location. In addition, to meet surges in demand the authority may need to reach contractual agreements with suppliers for emergency orders, which may be limited by the maximum production rate of α units per day during a pandemic. Since ventilators are durable, the stock of ventilators does not decrease over time due to usage. We assume that they can be deployed to different regions at negligible cost. Therefore, the total number of available ventilators in the entire alliance is given by $K_j = K_0 + \alpha j$, on the j-th day since the onset of the pandemic. Hence, the only decision variable of the central authority in the case of ventilators is the initial stockpile size K_0. Since ventilators are durable, there will be a considerable idle stockpile, which can be repurposed after the pandemic ends. This paper focuses on the resource management during the course of the pandemic, and thus repurposing is not being considered herein.

Figure 6: Two extreme scenarios of initial stockpile size K_0 for ventilators

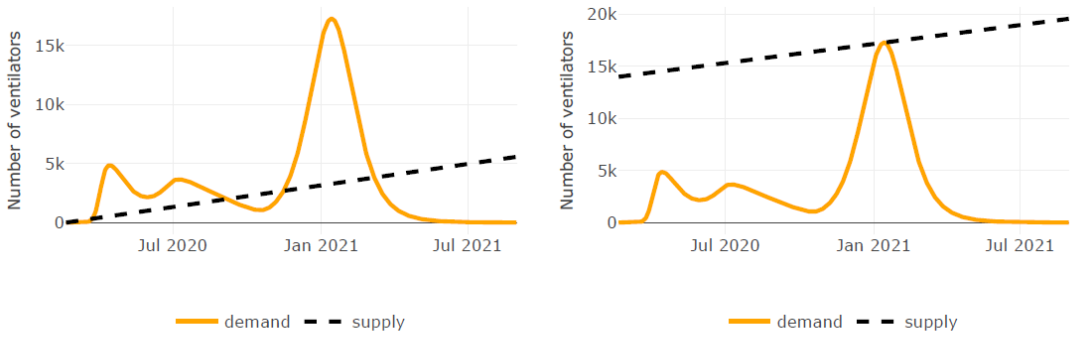

(a) Extreme understocking

(b) Extreme oversupply

To better explain the need for an optimal initial stockpile size K_0, consider two extreme cases in Figures 6a and 6b for the three-state alliance. On one end of the extreme, the central authority may decide to not hold any initial stockpile but simply rely on the maximum emergency production limit during the pandemic; Figure 6a shows clear severe shortages at all peaks of aggregate ventilator demand, and this is especially so around January 2021. On the other end, suppose that the central authority decides to hold an extraordinary amount of initial stockpile for ventilators to meet the highest peak of aggregate ventilator demand; Figure 6b illustrates a clear extreme oversupply of ventilators during most of the time of the pandemic; also, in this case the economic cost of severe over-storage can be huge. Therefore, the central authority has to take a delicate balance on an initial stockpile size K_0 that takes into account the economic cost of shortage and oversupply, as well as storage costs.

Consider the following optimization model for an initial stockpiling size.

$$\min_{K_0 \geq 0} \sum_{j=1}^{m} \omega_j \left(\frac{\theta_j^+}{2} \left(X_j^{\mathrm{VEN}} - (K_0 + aj) \right)_+^2 + \frac{\theta_j^-}{2} \left(X_j^{\mathrm{VEN}} - (K_0 + aj) \right)_-^2 + c_j \left(K_0 + aj \right) \right) + c_0 K_0, \qquad (1)$$

where m is the number of days of the pandemic, ω_j is a weight for significance of precision for the costs on the j-th day of the pandemic, θ^+ is an economic cost per squared unit of shortage, θ^- is an opportunity cost per squared unit of oversupply, c_j is the aggregate cost of possession per unit of ventilators per day, and c_0 is the initial stockpile cost, which may include both the acquisition cost and expected cost of possession (storage, maintenance, inventory logistics, opportunity cost). The quadratic form represents the real economic cost of supply–demand imbalance. For example, the first term is the product of the *quantity* of shortage

$$X_j^{\mathrm{VEN}} - (K_0 + aj)_{+\_}$$

and the (linear) *variable cost per unit* of the shortage

$$(\theta_j^{\pm}/2)[X_j^{\mathrm{VEN}} - (K_0 + aj)]_{+\ \_}.$$

In other words, the larger the shortage, the higher the economic price to pay. As opposed to an absolute value of shortage or surplus, the quadratic form arguably better reflects the economic

impact of demand–supply imbalance, whose real economic cost should be understood by the law of demand. Another interpretation is that a severe imbalance can have a ripple effect on the society, such as causing public panic and erosion of trust in the government's ability for crisis management, which requires additional cost for damage control. Therefore, the economic cost grows with imbalance in a non-linear fashion. For the same reason, we shall incorporate similar quadratic forms in the PPE contingency-planning problem as well as the resource-allocation problems in later sections below. The weight ω_j can be used for different purposes. For example, it may be reasonable to assume that the precision of meeting demands in the near future is more important than that in the far future given the uncertainty with prediction. Another case may be to make the weight proportional to the daily demand X_j as the demand–supply imbalance can have a greater impact on population-dense areas than otherwise. If life-saving is an overriding goal, then one can set the opportunity cost of oversupply θ^- to be zero. In practice, we could measure θ^+ and θ^- by regressing reported shortage or oversupply against estimated loss in gross domestic product or other economic measures during a pandemic.

Figure 7: Optimal initial stockpile K_0 relative to projected shortages without initial stockpile

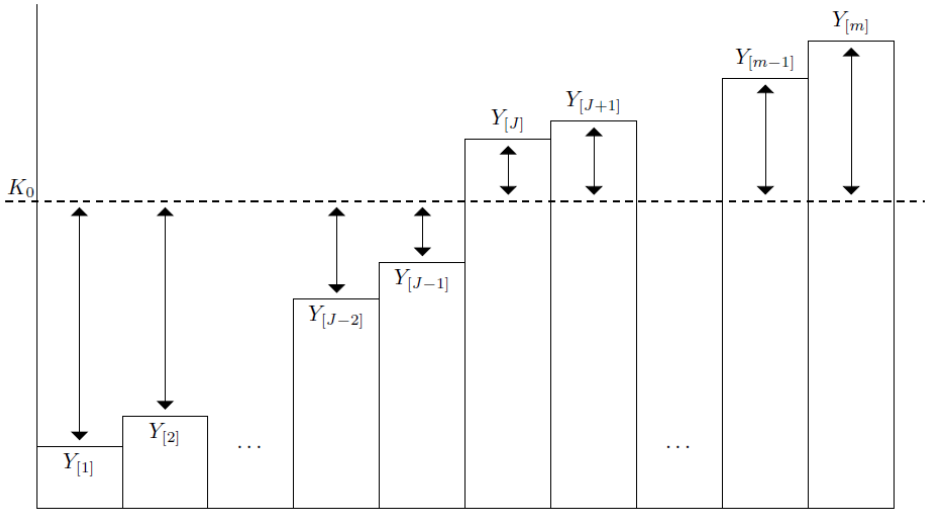

To understand the analytical solution to this problem, we need to look at the projected shortage without any initial stockpile, $Y_j := X^{\text{VEN}} - aj$, for $j = 1, \ldots, m$, which is the accumulated demand less the accumulated supply apart from the initial stockpile. Note that we consider the accumulated supply because the resources are durable and can be reused. When $Y_j > 0$, there is a drain on the initial stockpile as current demand exceeds the accumulated supply. Otherwise, the stockpile increases as supply exceeds demand. Because the economic costs of shortage and surplus are weighed differently, the value of this objective function depends on the number of days with a decreasing stockpile ($Y_j > 0$) and those with an increasing stockpile ($Y_j < 0$). The analytical solution to this problem requires the sorting of projected shortages in ascending order. Let us denote the sorted sequence by $\{Y_{[j]}, j = 1, \ldots, m\}$, where $Y_{[j]}$ represents the j-th smallest projected shortage. In the objective function (1), the cost coefficient $\theta_j^{\pm}$ applies according to whether or not stockpile exceeds demand. If K_0 is placed below $Y_{[j]}$, there is a shortage in the healthcare system and hence the cost coefficient θ^+ is applied. Otherwise,

there is a surplus in the system and the cost coefficient θ^- is applied. The optimality is achieved when K_0 is kept at a delicate position (see Figure 7). The nature of the sum of squared shortages in (1) determines that the optimal initial stockpile K_0^* should be squeezed between $Y_{[J-1]}$ and $Y_{[J]}$ in such a way that

$$Y_{[J-1]} \leq \frac{\sum_{j=1}^{J-1} \omega_{[j]}\theta_{[j]}^{-}\left(Y_{[j]} - \frac{c_{[j]}}{\theta_{[j]}^{-}}\right) + \sum_{j=J}^{m} \omega_{[j]}\theta_{[j]}^{+}\left(Y_{[j]} - \frac{c_{[j]}}{\theta_{[j]}^{+}}\right) - c_0}{\sum_{j=1}^{J-1} \omega_{[j]}\theta_{[j]}^{-} + \sum_{j=J}^{m} \omega_{[j]}\theta_{[j]}^{+}} \leq Y_{[J]}.$$

Once J is identified, the optimal stockpile K_0^* is given by

$$K_0^* = \max\left\{\frac{\sum_{j=1}^{J-1} \omega_{[j]}\theta_{[j]}^{-}\left(Y_{[j]} - \frac{c_{[j]}}{\theta_{[j]}^{-}}\right) + \sum_{j=J}^{m} \omega_{[j]}\theta_{[j]}^{+}\left(Y_{[j]} - \frac{c_{[j]}}{\theta_{[j]}^{+}}\right) - c_0}{\sum_{j=1}^{J-1} \omega_{[j]}\theta_{[j]}^{-} + \sum_{j=J}^{m} \omega_{[j]}\theta_{[j]}^{+}},\ 0\right\}.$$

The proof of this result can be found in Appendix A.1. This result shows that the optimal initial stockpile K_0 is the weighted average of all projected shortages discounted by the cost of possession relative to the economic cost of shortage, $Y_{[j]} - c_{[j]}/\theta_{[j]}^{\pm}$. The adjustment term $c_{[j]}/\theta_{[j]}^{\pm}$ indicates that the higher the cost of possession relative to the economic cost of imbalance, the fewer ventilators should be acquired. It is logical that if the cost of possession for durable resources is too high, the central authority in a poor country may have little financial means to pay for stockpiling and be left with no choice but to deal with the demand–supply imbalance. In contrast, if the economic cost of imbalance is too high due to lost productivity or even the society's resentment regarding the government's failure to meet demand, then the central authority would ignore the cost of possession and do everything possible to reduce the shortage.

Figure 8: Optimal initial stockpile size K_0 for ventilators according to different weights of economic cost

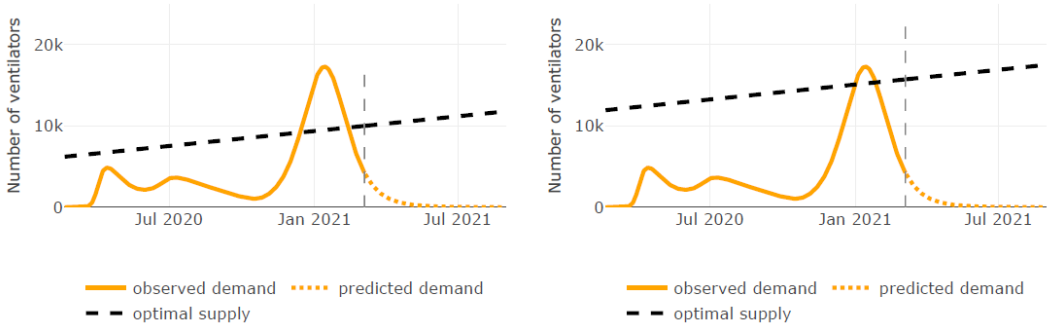

(a) $\theta_j^+ = \theta_j^-$ (Shortage costs the same as surplus)

(b) $\theta_j^+ = 20\theta_j^-$ (Shortage costs more)

Figure 8 depicts the optimal initial stockpile size in the case study. The model parameters are provided in Appendix B. Observe that optimal initial stockpiles are chosen to reduce shortages in the early stage and oversupply in the late stage of the pandemic, compared with those strategies shown in Figure 6. When the resource shortage costs the same or less than the

resource surplus, Figure 8a shows that the strategy requires less initial stockpiling due to the excessive amount of supply after the pandemic dies down. In contrast, if the shortage costs more than the surplus, the strategy is to reduce shortages in the early stage at the expense of increasing oversupply in late stages; see Figure 8b.

3.2 Single-Use Resources: Personal Protective Equipment

Similar to the case of durable resources, the central authority needs to set up an initial stockpile size K_0 of single-use resources such as PPE and make contractual agreements with emergency suppliers, which can provide additional supply at the production rate a units per day. Since PPE is single-use, during the pandemic the central authority has to stockpile PPE sets not only for the present but also for potentially deploying them at a later time in order to meet a surge in demand. Therefore, the central authority needs to plan for both the initial stockpile size K_0 and the amount of distribution k_j to all regions on day j. The dynamics of the centralized storage $\{K_j, j = 0, 1, \ldots, m\}$ are determined by the recursive relation $K_j = K_{j-1} + a - k_j + (k_j - X_j)_+$ for $j = 1, \ldots, m$. The relation can be interpreted as follows. The current stockpile K_j is based on the previous period's stockpile K_{j-1}, increased by the net surplus of new supply a less the arranged distribution up to the total demand, $\max\{k_j, X_j\}$. In other words, if we arrange to distribute k_j units but can only consume $X_j < k_j$, then the unused amount should count towards the centralized storage for future use.

Figure 9: Two extreme scenarios of distribution schedule $k_1, k_2, \ldots, k_m$ for PPE

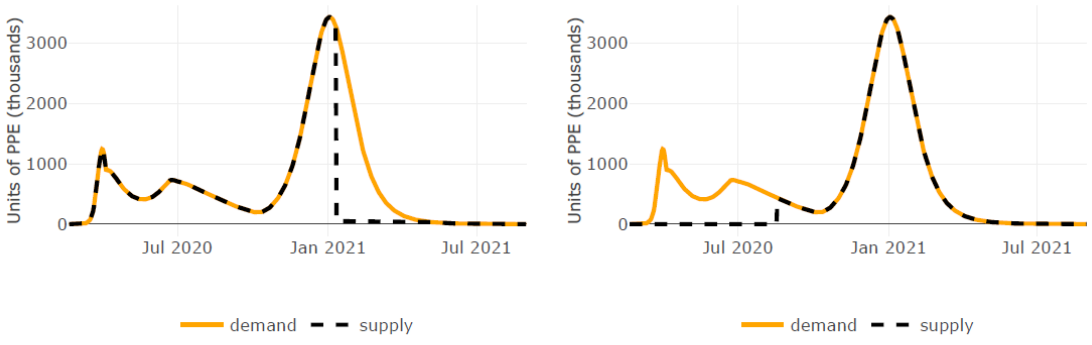

(a) Aggressive distribution

(b) Conservative distribution

Consider two extreme cases in Figures 9a and 9b in the case study. In an extreme case, assume that the central authority decides to distribute as much as possible to meet the demand until the centralized storage is exhausted. This aggressive early-distribution strategy is depicted in Figure 9a. After the storage depletion, the system relies only on the new supply, which clearly is not sufficient to meet demands and can cause severe shortages near the peak in January 2021. In the other extreme case, the central authority may choose to hold off dispersing any equipment at all till the point that the storage is believed to be sufficient to cover all future demands. Such a conservative distribution strategy is illustrated in Figure 9b. The challenge with this strategy is that the central authority would have to deal with the repercussions of not providing any assistance in the early stage of the pandemic. Therefore, it is sensible that the

central authority develops a distribution schedule that takes a temporal balance of varying needs from all regions. Here we introduce the optimization problem for both an initial stockpile and the distribution schedule of single-use resources.

$$\min_{K_0 \geq 0, k_1, \ldots, k_m} \sum_{j=1}^{m} \omega_j \left(\frac{\theta_j^+}{2} \left(X_j^{\mathrm{PPE}} - k_j \right)_+^2 + \frac{\theta_j^-}{2} \left(X_j^{\mathrm{PPE}} - k_j \right)_-^2 + c_j K_j \right) + c_0 K_0 \tag{2}$$

$$\text{such that } K_j = K_{j-1} + a - k_j + \left(k_j - X_j^{\mathrm{PPE}} \right)_+ \geq 0 \text{ and } k_j \geq 0, \quad \text{for } j = 1, 2, \ldots, m,$$

where c_j is the centralized cost of possession per unit of PPE per day. It should be pointed out that the centralized storage should be kept non-negative for practical purposes and the distribution amount should also be kept non-negative.

Figure 10: Optimal distribution schedule k_1, k_2, …, k_m and initial stockpile size K_0 of PPE for the three-state resource-pooling alliance

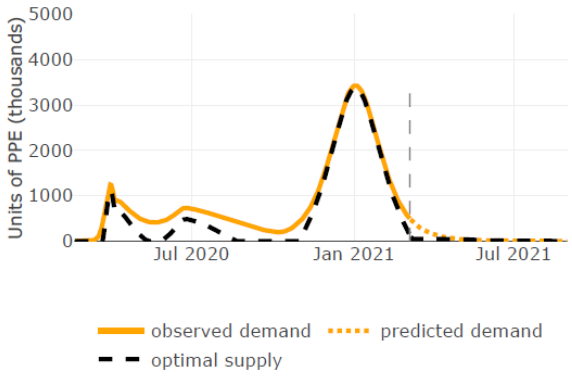

Figure 10 depicts the case of an optimal distribution schedule for the three-state alliance. Observe that the optimal supply distribution schedule stays below the trajectory of demand. The slight shortage results from the consideration of the cost of possession. Should the cost of possession be zero, the optimal supply would be to match the demand exactly at all times. The initial stockpile can be set artificially high so that any desired amount can be carried over from period to period and last long enough to support all future demands. In the presence of possession cost, Figure 10 also reveals a distribution strategy that in essence ignores the demands at the start of a pandemic and after the pandemic dies down, and instead focuses on meeting demands at the first peak of the pandemic. Keep in mind that the weight of significance ω_j in this example is set to be proportional to the size of demand. Therefore, the strategy prioritizes meeting the demand in the first peak over other periods due to its high demand. If we were to choose the same weight ω_j for all periods, the shortage would be more balanced among all periods.

This optimization problem is cumbersome to be solved analytically. However, it is straightforward to show that any oversupply distribution scheme $k_j > X^{\mathrm{PPE}}$ must be sub-optimal, and hence the problem can be simplified as follows:

$$\min_{K_0 \geq 0, k_1, \ldots, k_m} \sum_{j=1}^{m} \omega_j \left(\frac{\theta_j^+}{2} \left(X_j^{\mathrm{PPE}} - k_j \right)^2 + c_j K_j \right) + c_0 K_0$$

such that $K_j = K_{j-1} + a - k_j \geq 0$ and $0 \leq k_j \leq X^{\mathrm{PPE}}$, for $j = 1, 2, \ldots, m$.

Because of the convexity, it can be solved numerically using Disciplined Convex Programming (DCP), which requires minimal computational time (Grant, Boyd, and Ye, 2006). The solution shown in Figure 10 is obtained with the help of an R package, CVXR, developed based on the DCP method (Fu, Narasimhan, and Boyd, 2020).

4. Pillar III: Centralized Resources Allocation

In the time of severe resource shortages, a coordinated effort becomes necessary to obtain additional supplies and to ration limited existing resources. Existing resources are not necessarily distributed on a basis of health need or justice (Tobin-Tyler, 2020). Many hardest-hit states have to ration care, while other states have low utilization of their resources. As alluded to earlier, not all regions experienced surges in demand at the same time (see Figure 2). It has long been argued that the US federal government should have tracked the current use and the projection of needs in all states, and coordinated the allocation of resources to reduce shortages across regions and over time during the COVID-19 pandemic (Ranney, Griffeth, and Jha, 2020).

There are two common types of resource-allocation problems in the course of a pandemic, both of which can be formulated and cast in Pillar III of our proposed framework:

1. *Macro-level resources pooling*. A central authority acts in the best interest of a union of many regions to increase supply and coordinate the distribution of existing and additional resources among different regional healthcare providers.
2. *Micro-level rationing*. Facing an imbalance of demands and supplies in medical equipment and resources, hospitals often have to make difficult but necessary decisions to ration limited existing resources as well as new supplies.

While in both cases the aim of allocation is to deliver limited resources to where they are needed the most, the macro-level pooling largely addresses spatio-temporal differences, and the micro-level rationing focuses on healthcare effectiveness and justice. The setting of standards, protocols, and policies can have a profound impact on the functioning of a healthcare system at the time of crisis. Therefore, the best practice of resources allocation should be based on scientific assessment and evaluation rather than on-the-fly ad hoc decisions and a patchwork of damage-control rules.

1. *Resources allocation should be based on a holistic approach to address concerns of all stakeholders.* There are often conflicting interests and priorities for using limited resources. For example, when medical supplies are scarce, many countries, states, and cities are competing for resources. While each state acts in its best interest to acquire medical devices and protective equipment, a federal government may see the urgent need to seize control of the cargo to boost a centralized stockpile. A holistic approach aims to strike a balance among different objectives for various stakeholders.
2. *Scientific methods for resources allocation should be developed under a set of optimization objectives, meet certain ethical and humanitarian criteria, and take into account logistic and budgetary constraints.* When a pandemic breaks out, it often spreads from one cluster to another in geographic areas due to its transmission dynamics and affects different sectors of a healthcare system in a chain reaction. Medical needs can vary greatly by demographics and other socio-economic factors. While there is no universal “one-size-fits-all” solution for allocation problems, there are a set of quantifiable and justifiable criteria.

While it is difficult to address all of these criteria in a single model, we believe that they can be formulated similarly, as in this section.

- **Minimization of shortage and oversupply**

  Decision makers need to take into account spatio-temporal differences in demand and supply over the course of a pandemic. It is imperative for authorities to allocate more resources to epicenters of a pandemic than other regions under less imminent threat. For example, New York City was the first in the State of New York to witness the COVID-19 pandemic, when other counties had few to no reported cases (Associated Press, 2020). The state governor issued an executive order to take ventilators and other protective gear from underutilized private hospitals and companies. As infected cases stabilize or even decline in pandemic-ravaged regions, a central authority may need to shift its attention to other areas of potential outbreaks and allocate resources in anticipation of new waves. This was also evident when many states in the United States in the early stages of the COVID-19 outbreak took pre-emptive measures to procure medical supplies from countries like China and South Korea which had developed production capacities after the local epidemics were under control. Therefore, it is sensible to develop an allocation strategy that minimizes shortages and oversupply across different regions and over the life-cycle of a pandemic.

- **Promoting and rewarding instrumental value**

  Critical preventive gear and medical care should be provided first to healthcare workers in the front line, and employees in essential businesses and critical infrastructure. Not only because they are at high risk due to their exposure to infectious disease, but also because the society bears a heavy economic cost when these workers fall ill and are unable to return to work. The lack of a sufficient front-line workforce may cause severe disruptions to public services, which can have a rippling effect on the rest of the economy. Priority access to medical care can be a critical incentive for retention.

- **Prioritizing the worst-off**

  The ultimate goal of a healthcare system is to save lives. Access to critical medical treatment should be reserved for patients facing life-threatening conditions when there is an insufficient supply of equipment such as ventilators.

- **Maximization of benefit from treatment**

  Maximization of the benefit requires a prognosis on how patients are likely to survive with treatment. A recent study of COVID-19 patients in the United States found that most patients did not survive after being placed on mechanical ventilators (Preidt, 2020). To maximize the benefit, access to ventilator treatment should be prioritized for younger patients who can benefit the most and have a higher chance of survival. For example, many hospitals in Italy lowered the age cut-off from 80 to 75 in order to ration limited ventilators (Rosenbaum, 2020). Such a strategy often leads to ethical dilemmas when in conflict with prioritizing the worst-off.

The third pillar of the proposed pandemic risk management framework is to allocate limited resources for different regions, building on the proposed optimal centralized stockpiling and distribution strategies. Figures 11a and 12a put the regional resources demand and optimal aggregate supply together for the ease of exposition.

Figure 11: Optimal ventilator allocations in New York, Florida, and California

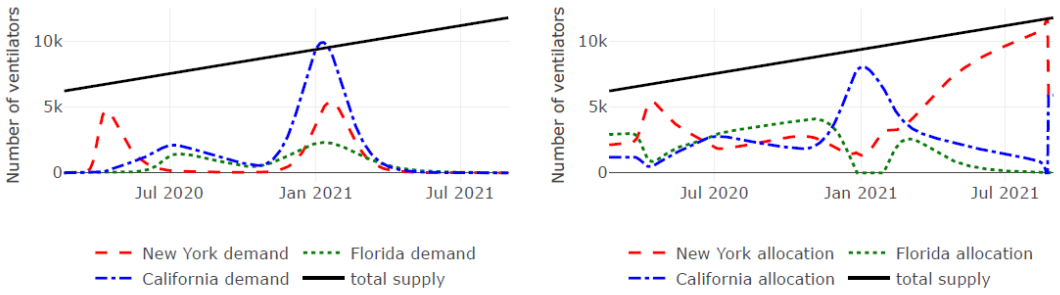

(a) Regional ventilator demands (b) Optimal ventilator allocations

Figure 12: Optimal PPE allocations in New York, Florida, and California

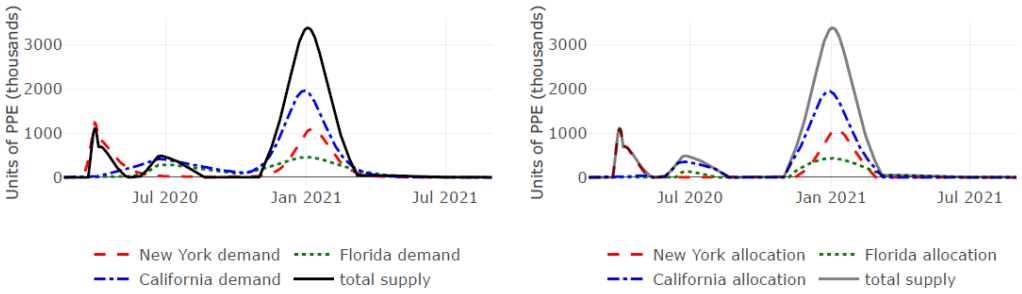

(a) Regional PPE demands (b) Optimal PPE allocations

4.1 Durable Resources: Ventilators

Throughout this section we consider the allocation of existing resources in a healthcare system with *n* regions during a pandemic that lasts for *m* days. We always use the superscript (*i*) to indicate quantities for the *i*-th region. Bear in mind that there could still be an aggregate shortage of supply for ventilators and PPE sets to all regions in the alliance. The central authority would have to take a holistic view of competing interests of participating regions. On each day in the pandemic, when the aggregate demand exceeds the aggregate supply, the central authority should choose to allocate resources taking into account spatial differences in demand and supply. This motivates the optimization model for ventilator allocations:

$$\min_{\substack{K_j^{(i)}\geq 0; i=1,2,\ldots,n; \\ j=1,2,\ldots,m}} \sum_{j=1}^{m}\sum_{i=1}^{n} \omega_j^{(i)} \left(\frac{\theta_j^{+(i)}}{2} \left(X_j^{\mathrm{VEN}(i)} - K_j^{(i)} \right)_+^2 + \frac{\theta_j^{-(i)}}{2} \left(X_j^{\mathrm{VEN}(i)} - K_j^{(i)} \right)_-^2 \right)$$

$$\text{such that } \sum_{i=1}^{n} K_j^{(i)} = K_j, \quad \text{for } j = 1, 2, \ldots, m,$$

where $\omega^{(i)}$ is a weight to the *j*-th day of the pandemic in the *i*-th allied region, $\theta^{+(i)}$ is an economic cost per squared unit of shortage, and $\theta^{-(i)}$ is an opportunity cost per squared unit of oversupply. The quadratic term $\theta^{\pm(i)}/2\ X^{(i)} - K^{(i)}$ represents the economic cost due to the demand–supply imbalance. Note that $\theta^{\pm(i)}/2$ measures the rate of increase in cost per unit, and hence $\theta^{\pm(i)}/2\ X^{(i)} - K^{(i)}$ represents the linear variable cost per unit. The variable cost in principle reflects the law of demand that the price increases with the quantity demanded. Therefore, the total cost is the product of variable cost per unit $\theta^{\pm(i)}/2\ X^{(i)} - K^{(i)}$ and the total unit of imbalance $X^{(i)} - K^{(i)}$. The economic cost is used to account for both potential loss of life due to the lack of resources and the opportunity cost of idle medical sources due to oversupply. The structure of economic cost is used not only for its mathematical tractability, but also to penalize large imbalances of demand and supply. The weight $\omega^{(i)}$ can be used to measure the relative importance of resource allocation for region i at time t_j to other regions and time points. There are some examples of its application under various criteria for resource-pooling or resource-rationing. For example, in a national contingency plan, where $X^{(i)}$ is used as the predicted demand from each region, for political reasons a metropolitan area with a large population may carry more weight than a rural area with a small population. When hospitals have to ration limited resources, they may implement the strategy to maximize the benefit from treatment. In such a set-up, $X^{(i)}$ represents the demand from a particular cohort. A decision maker may give higher weight to age cohorts with more remaining life years than age cohorts with fewer remaining years. It is also a common strategy to give priority for access to medical resources to healthcare workers. In both cases, the set of weights $\omega^{(i)}$ reflects the management's priorities and preferences over time. Some specific choices of the weights $\omega^{(i)}$ can also reflect demographic characteristics. For example, if a region, say i, has a comparatively larger population of elderly people who are more susceptible to the pandemic, then the epidemic compartmental models, such as the aforementioned SEIRD model, would project a higher demand $X^{(i)}$. In this case, when the regional weight $\omega^{(i)}$ is set to be monotonic with respect to the projected regional demand $X^{(i)}$, then a higher priority will spontaneously be given to the region i's quadratic term of economic cost.

The constraint $K^{(i)} = K_j$ indicates that resources allocated to different regions must add up to the total amount of supply available to the central authority. The evolution of supply $\{K_j, j = 1, 2, \ldots, m\}$ is based on the centralized stockpiling strategy discussed in previous sections. The evolution of demand $\{X_j, i = 1,\ldots, n, j = 1, 2, \ldots, m\}$ can be based on forecasts from epidemiological models fitted to the most recent local data.

4.2 Single-Use Resources: Personal Protective Equipment

The allocation of single-use resources is similar to that of durable resources. The key difference lies in the amount of the stockpile to be released each period. For durable resources, the central authority distributes the accumulated stock K_j at any given time *j*. Because single-use resources cannot be reused, the central authority can only distribute incremental amounts according to some distribution schedule. With this difference in mind, we formulate the allocation of single-use resources by an optimization problem.

$$\min_{\substack{k_j^{(i)}\geq 0; i=1,2,\ldots,n; \\ j=1,2,\ldots,m}} \sum_{j=1}^{m}\sum_{i=1}^{n} \omega_j^{(i)} \left(\frac{\theta_j^{+(i)}}{2} \left(X_j^{\mathrm{PPE}(i)} - k_j^{(i)} \right)_+^2 + \frac{\theta_j^{-(i)}}{2} \left(X_j^{\mathrm{PPE}(i)} - k_j^{(i)} \right)_-^2 \right)$$

$$\text{such that } \sum_{i=1}^{n} k_j^{(i)} = k_j, \quad \text{for } j = 1, 2, \ldots, m.$$

Note that the distribution amount k_j could be determined prior to a pandemic by some contingency planning or during a pandemic by an adjusted distribution schedule. Section 3.2 "Single-Use Resources: Personal Protective Equipment" offers an example of how such a distribution schedule can be determined to take into account temporal competition for single-use resources.

4.3 Holistic Allocation Algorithms

The analytical solutions to allocation problems regarding both durable and single-use resources can be derived in the same way for the reason that they essentially take the same form. Hereinafter, because the allocation is done from period to period in the solution, we shall suppress the subscript *j* for brevity. To simplify notation in the solution, we will use $X^{(i)}$ without the indicator of resource type for the demand in region *i*, and use $K^{(i)}$ for the quantity of allocated resources in region *i*.

Here we discuss the analytical solutions to the optimization problems presented above, from which we can glean economic insights. The proofs of these solutions are given in Appendix A.2.

The central authority has to first determine whether or not there is a system-wide surplus or shortage. The allocation strategy differs under these scenarios.

It is worth pointing out that, in either scenario, the pandemic resource-allocation problem is in essence a model of Pareto optimality with regard to competing interests of members in a group. Pareto optimality is a widely accepted concept used to study economic efficiency for finite resources allocation. The optimality is attained when there is no alternative allocation which can improve the welfare of some members without worsening that of other members. The solution based on such an optimality might result in an allocation being sub-optimal to certain members; yet the Pareto optimal allocation minimizes the overall objective as a group. The allocation problem that involves members with competing interests has been extensively studied in Chong, Feng, and Jin (2021), and we will borrow some ideas from that work to make economic interpretations of the results of allocation models here. In addition, as a matter of fact, one could also perceive those optimization problems in the "Pillar II: Centralized Stockpiling and Distribution" section being formulated as self-Pareto optimality across time.

System-wide Surplus

If there is an overall surplus in the healthcare system at time *j* (i.e., $K > \sum_{r=1}^{n} X^{(r)} = X$, then only the economic cost for oversupply $\theta^{-(i)}$ applies and the optimal allocation of existing supply to the i-th region is given by

$$K^{(i)} = \left(1 - \frac{\frac{1}{\omega^{(i)}\theta^{-(i)}}}{\sum_{r=1}^{n} \frac{1}{\omega^{(r)}\theta^{-(r)}}}\right) X^{(i)} + \frac{\frac{1}{\omega^{(i)}\theta^{-(i)}}}{\sum_{r=1}^{n} \frac{1}{\omega^{(r)}\theta^{-(r)}}} \left(K - \sum_{r \neq i} X^{(r)}\right), \forall i = 1, 2, \cdots, n. \tag{3}$$

Observe that the allocation formula (3) has an explicit economic interpretation, which shows that the optimal supply for region *i* results from a balance of two competing optimal solutions:

- **Self-concerned optimal supply: $X^{(i)}$**

  If region *i* can ask for as much as it needs, then this amount shows the ideal supply in the best interest of the region alone. The demand and supply for all other regions are ignored in its consideration.

- **Altruistic optimal supply:** $K - \sum_{r=1; r \neq i}^{n} X^{(r)}$

  If the region *i* places the interests of all other regions above its own, then the medical supply goes to other regions and region *i* ends up with the leftover amount.

The central authority has the responsibility of mediating among regions competing for resources. The formula indicates that the optimality for region *i* in consideration of the entire system is the weighted average of two extremes, namely the self-concerned optimal and the altruistic optimal supplies. It should be pointed out that the average of two optimal supplies is determined by the harmonic weighting $\frac{1}{\omega^{(i)}\theta^{-(i)}} \Big/ \sum_{r=1}^{n} \frac{1}{\omega^{(r)}\theta^{-(r)}}$ as opposed to arithmetic weight $\omega^{(i)}\theta^{-(i)} \Big/ \sum_{r=1}^{n} \omega^{(r)}\theta^{-(r)}$. It is known in Chong, Feng, and Jin (2021) that in multi-objective Pareto optimality the harmonic weighting is always used for balancing competing interests of participants in a group, whereas the arithmetic weighting serves the purpose of balancing competing objectives of the same participant.

An alternative interpretation of formula (3) can be obtained from the equivalent formula

$$K^{(i)} = X^{(i)} + B^{(i)} \left(K - \sum_{r=1}^{n} X^{(r)}\right), \qquad B^{(i)} = \frac{\frac{1}{\omega^{(i)}\theta^{-(i)}}}{\sum_{r=1}^{n} \frac{1}{\omega^{(r)}\theta^{-(r)}}}. \tag{4}$$

It follows from (4) that the allocated resource is always presented as an adjustment to the actual demand. When there is a surplus in the system supply after optimal supplies have been distributed to all regions in order to fully meet their demands, then additional resources can be made available for region *i* and each region obtains a portion determined by harmonic weighting. Observe that $\sum_{i=1}^{n} K^{(i)} = K$ as expected since $\sum_{i=1}^{n} B^{(i)} = 1$.

System-wide shortage

If there is an overall shortage in the healthcare system at time *j* (i.e., $K \leq \sum_{r=1}^{n} X^{(r)} = X_{\cdot}$), it turns out that the optimal allocation strategy is to deliver the resources where they are needed the most. We can summarize the algorithm in three steps:

- **Step 1: Demand ranking**

  The first order of business is to sort regional demands $\{X^{(i)},\ i = 1, \ldots, n\}$ in a descending order. We use the subscript $[i]$ to indicate the i-th largest order statistic; i.e., $X^{[1]} \geq \ldots \geq X^{[n]} \geq 0$. The ranking of regional demands determines the order in which the regions are considered for resources allocation in the next step.

- **Step 2: Frugality test**

  The algorithm first tests cases that perform allocation rules in a similar way to (4). For any fixed $I = 1, \ldots, n$, consider the holistic allocation rule that provides for I regions with largest demand by

$$\tilde{K}^{[i]} = X^{[i]} + \tilde{B}^{[i]} \left(K - \sum_{r=1}^{I} X^{[r]} \right), \qquad \tilde{B}^{[i]} = \frac{\frac{1}{\omega^{[i]}\theta + [i]}}{\sum_{r=1}^{I} \frac{1}{\omega^{[r]}\theta + [r]}}. \tag{5}$$

  To find the optimal number I of regions to support, the algorithm ensures that the allocation rule should be frugal to meet the following criteria:

  1. The total supply K is only almost enough to meet the demands for all I regions;

$$K \leq \sum_{r=1}^{I} X^{[r]}.$$

  2. When the allocation rule (5) is forcefully applied to all regions, the I regions with highest demands should receive non-negative allocation and the rest of the group negative allocation.

$$\tilde{K}^{[1]}, \cdots, \tilde{K}^{[I]} \geq 0 > \tilde{K}^{[I+1]}, \cdots, \tilde{K}^{[n]}.$$

  There is a unique value of I that passes the frugality test. As the aim of the strategy is to cover as many regions of highest demand as possible, the search algorithm stops after the total demand of I regions exceeds the available supply. The algorithm would reach a rule that can be rewarding for those I regions but discourages allocations to the rest.

- **Step 3: Holistic allocation**

  Once the algorithm settles on the value of I, all existing resources are divided among the I states according to the holistic allocation principle. In other words, the allocation of supply to the *i*-th region is given by

$$K^{[i]} = \tilde{K}^{[i]}, \qquad \forall i = 1, 2, \cdots, I;$$
$$K^{[I+1]} = \cdots = K^{[n]} = 0.$$

The general idea of the holistic allocation is illustrated in Figure 13. The first row in the figure shows that when there is a system-wide shortage, the total demand in all I regions $\sum_{i=1}^{I} X^{[i]}$ can be viewed as the composition of the total supply *K* and the shortage $Y := \sum_{i=1}^{I} X^{[i]} - K$. Therefore, in the process of regional allocation, those I regions need to not only share the total available resources, but also jointly carry the burden of shortage, which is in proportion to their respective harmonic weight $\tilde{B}^{[i]}$, for $i = 1, 2, \ldots, I$. Therefore, each region receives its demand less its "fair" portion of the system-wide shortage; i.e., $X^{[i]} - \tilde{B}^{[i]}Y$. For example, the amount of resources allocated to region *i* is $K^{[1]}$ and the shortage to be shared is given by $\tilde{B}^{[1]}Y$, which is represented by the stippled area in Figure 13. Those two parts add up to the total demand in that region; i.e., $X^{[1]}$. One could argue that a limitation of this solution is that there is no resource allocated to regions $I + 1$ to *n* and it would be unreasonable for ethical reasons. Such an issue can be addressed by setting some minimal amount of allocation in each region. This can be easily incorporated by extending the optimization model with additional constraints that $K_j^{(i)} \geq M_j^{(i)}$ for $i = 1, 2, \ldots, n,$ and $j = 1, 2, \ldots, m,$ where $M_j^{(i)}$ is some minimal supply mandated by policymakers.

The solutions to the three-state alliance for pooling ventilators and PPE sets are shown in Figures 11b and 12b. Figure 11b depicts the case of optimal allocation strategies for ventilators, which confirms the intuition in the "Case Study" section. In April 2020, the central authority could have optimally reallocated all available aggregate ventilators in the alliance to New York. This is owing to the fact that New York has the highest demand of all three states. By May and June 2020, ventilators in New York could have been gradually reallocated to both Florida and California; in July and August 2020, with the reallocated resources from New York, both Florida and California should have experienced no shortage of ventilators at all. In January 2021, when there is another rapid surge of demand, the supply of ventilators is shifted from the relatively less impacted states (i.e., New York and Florida) to California, where the increase in demand is extraordinary.

Figure 13: Holistic allocation of resources in the face of system-wide shortage

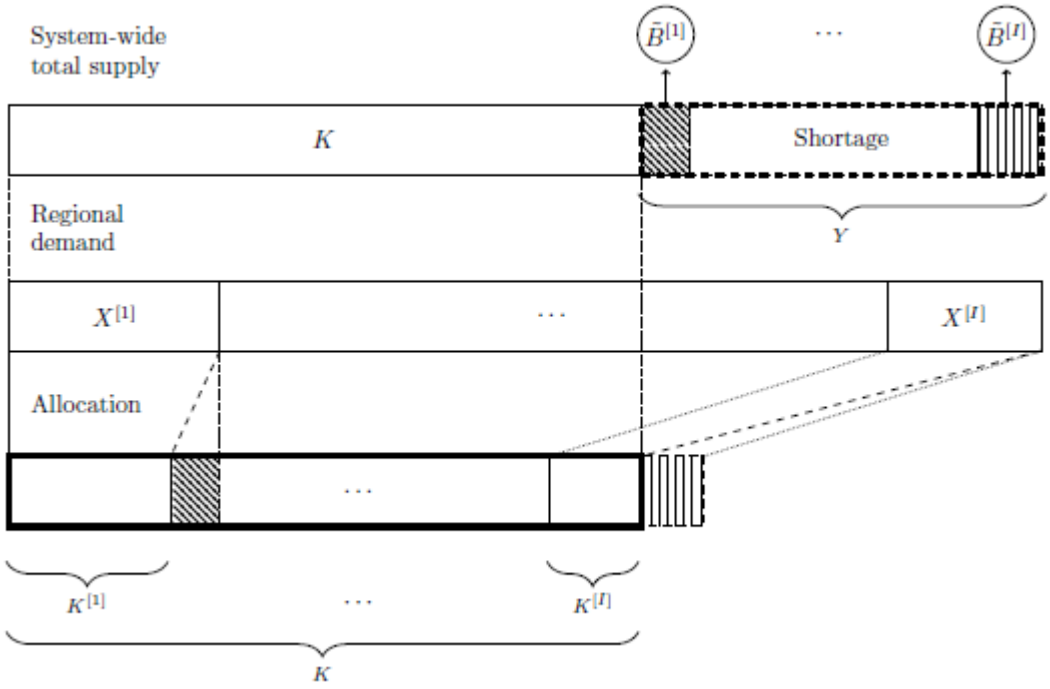

Figure 12b illustrates optimal allocation strategies for PPE sets in the case study. In April 2020, the central authority could distribute stockpiled PPE sets and have them all sent to New York for its emergency response. As the pandemic dies down for New York and picks up for California and Florida in June 2020, the resources are more evenly spread. In August 2020, once the shortage is contained in all three states with relatively little outstanding demand, the available PPE sets should be stashed in preparation for the simultaneously rising demands that peak in January 2021.

5. Adjustments in Real Time

As alluded to earlier, while this paper proposes the three-pillar framework, the three pillars should be utilized in a cycle. COVID-19 has taught us that a pandemic's progress is hard to predict. In the early stage of the outbreak, when there is little clinical data, Pillar I for resource-demand prediction is based on "best estimates" for epidemiological models available at the time. It is possible that the action planned, prior to a pandemic, in Pillars II and III could be sub-optimal during the pandemic. This section briefly discusses adjustments needed in the three-pillar framework in real time.

Suppose that at a certain time point in the pandemic, say l, for $0 < l < m$, the pandemic has not evolved as predicted by epidemiological models, where m could be an estimated end time of the pandemic. For Pillar I, the clinical parameters in the compartmental model, such as the transmission rate, can be recalibrated using the data collected from time 0 until time l. Moreover, the usage parameter of resources by each compartment also needs to be re-evaluated. These two updates together provide an up-to-date prediction on resources demand.

During the pandemic, there may be a need to readjust distribution strategies for single-use resources, as described in Section 3.2. If the previous distribution strategy was based on an overly liberal estimate of demand, an oversupply of single-use resources may cause waste in regions. If it was based on a conservative estimate, a shortage may occur. Therefore, it is critical for decision makers to recalibrate demand projections and feed them into the model for an optimal distribution strategy.

Suppose that the new demand projection is given by $\{\tilde{X}_{l+1}^{\mathrm{PPE}}, \cdots, \tilde{X}_{m}^{\mathrm{PPE}}\}$ according to the updated information. The production rate may have also been updated to $\tilde{a}$ per day. The current stockpile is known to be K_l. Then we reconsider the optimal distribution schedule

$$\min_{k_{l+1},\ldots,k_m} \sum_{j=l+1}^{m} \omega_j \left(\frac{\theta_j^+}{2} \left(\tilde{X}_j^{\mathrm{PPE}} - k_j \right)_+^2 + \frac{\theta_j^-}{2} \left(\tilde{X}_j^{\mathrm{PPE}} - k_j \right)_-^2 + c_j K_j \right)$$

$$\text{such that } K_j = K_{j-1} + \tilde{a} - k_j + \left(k_j - \tilde{X}_j^{\mathrm{PPE}} \right)_+ \geq 0 \text{ and } k_j \geq 0, \quad \text{for } j = l+1, l+2, \ldots, m.$$

Note that this optimization problem is the analogue of (2) with updated demand projections.

For Pillar III, based on the new prediction on resources demand, and the new distribution strategic plan for single-use resources, allocation strategies are updated by solving the optimization problem at each time, from *l* to *m*, formulated as before. In practice, this implies a *confiscation* of all resources held by all regions in the alliance for a complete reallocation.

Finally, the cycle of adjustments may be repeated periodically throughout the pandemic. The fundamental philosophy is that while we cannot change what happened in the past, we can make optimal decisions given current forecasts of the future.

6. Conclusions and Limitations

The COVID-19 pandemic has placed extraordinary demands and constraints on public healthcare systems, exposing many problems, such as the lack of adequate planning and coordination. This paper investigates what could have been done better to reduce the imbalance of medical resources demand and supply. Inspired by classical theory of risk aggregation and capital allocation, this paper proposes a three-pillar resources planning and allocation framework: demand forecast, centralized stockpiling and distribution, and centralized resources allocation. This paper further develops a novel spatio-temporal balancing of resources and can potentially be used by public policymakers as a quantitative basis for making informed decisions on planning, funding, and rationing of critical resources. While this paper demonstrates the numerical case study based on a hypothetical three-state alliance of California, Florida, and New York, for the illustration of the effectiveness of these strategies, these are also applicable to the collaboration among other regions across the globe.

It should be pointed out that the paper focuses on managerial insights that can be drawn from the optimization framework and its analytical solutions. There are two potential areas of improvement if a framework is adopted in practice. First, estimation errors of model inputs should be allowed and yet result in a robust confidence range of contingency planning and allocation. Second, stochastic compartmental models may be considered, while the optimization models can be extended to other risk measures such as expectation or value-at-risk, and could even include constraints with deviation measurement.

Moreover, there are admittedly a number of limitations in the hypothetical example of a three-state resources-pooling arrangement. The three states are chosen for the most drastic effects of planning and allocation of existing resources for the purpose of illustration. It is beyond the scope of this paper to consider the political reality that may prevent such arrangements. In theory, the methodology can be applied to the actual voluntary coalition formed by six northeastern states in the United States, although the coalition was formed largely to avoid price competition in government procurement. Another limitation of this example is the egalitarian approach to shortages in different regions, which ignores ethical issues that may arise from freely moving resources from one region to another. While it may be economically optimal to deliver all resources in the system to the place where they are needed the most, it may be politically challenging to leave other places with less severe shortages without support. A potential remedy would be to introduce additional constraints in the optimization problems that require some minimal support for each region.

7. Acknowledgments

This research is supported by the Canadian Institute of Actuaries (CIA). We would like to express our deepest gratitude to the CIA project oversight group members, Victor Wang, Adam Granville, Alex Ngo, Cindy Li, and Shlomit Jacobson, for providing insightful comments and suggestions that improved the manuscript. We would also like to thank Qingxuan Kong, Charan Sankaran, Annie Zheng, Xuan Lin, Erchi Wang, and other students in the Illinois Risk Lab at the University of Illinois at Urbana-Champaign for their valuable supportive work.

References

Acemoglu, Daron, Victor Chernozhukov, Iván Werning, and Michael D. Whinston (May 2020). *Optimal Targeted Lockdowns in a Multi-Group SIR Model*. Working Paper 27102. National Bureau of Economic Research.

Arentz, Matt, Eric Yim, Lindy Klaff, Sharukh Lokhandwala, Francis X. Riedo, Maria Chong, and Melissa Lee (Apr. 2020). "Characteristics and Outcomes of 21 Critically Ill Patients With COVID-19 in Washington State". In: *JAMA* 323.16, pp. 1612–1614.

Associated Press (Apr. 2020). "Cuomo Signs Order to Redistribute Ventilators as New York Coronavirus Cases Top 100,000". *Boston Globe*. Online. www.bostonglobe.com/2020/04/03/nation/cuomo-signs-order- seize-ventilators-hospitals-redistribute-them-hard-hit-areas/.

Bhatraju, Pavan K., Bijan J. Ghassemieh, Michelle Nichols, Richard Kim, Keith R. Jerome, Arun K. Nalla, Alexander L. Greninger, Sudhakar Pipavath, Mark M. Wurfel, Laura Evans, Patricia A. Kritek, T. Eoin West, Andrew Luks, Anthony Gerbino, Chris R. Dale, Jason D. Goldman, Shane O'Mahony, and Carmen Mikacenic (Mar. 2020). "Covid-19 in Critically Ill Patients in the Seattle Region: Case Series". In: *New England Journal of Medicine* 382, pp. 2012–2022.

Charpentier, Arthur, Romuald Elie, Mathieu Laurière, and Viet Chi Tran (2020). "COVID-19 Pandemic Control: Balancing Detection Policy and Lockdown Intervention under ICU Sustainability". In: *Math. Model. Nat. Phenom*. 15, pp. 57–99.

Chong, Wing Fung, Runhuan Feng, and Longhao Jin (Feb. 2021). "Holistic Principle for Risk Aggregation and Capital Allocation". In: *Annals of Operations Research.* CovidActNow (Mar. 2020). Online. https://covidactnow.org/.

Dhaene, Jan, Andreas Tsanakas, Emiliano A. Valdez, and Steven Vanduffel (Mar. 2012). "Optimal Capital Allocation Principles". In: *Journal of Risk and Insurance* 79.1, pp. 1–28.

Ellison, Ayla (Apr. 2020). "20 States to Face ICU Bed Shortages when COVID-19 Peaks, Analysis Finds". *Becker's Hospital Review*. Online. www.beckershospitalreview.com/patient-flow/20-states-to-face-icu-bed- shortages-when-covid-19-peaks-analysis-finds.html.

Estes, Clary (2020). "States Are Being Forced Into Bidding Wars To Get Medical Equipment To Combat Coronavirus". *Forbes*. Online. www.forbes.com/sites/claryestes/2020/03/28/states-have-are-being-forced-into-bidding-wars-to-get-medical-equipment-to-combat-coronavirus.

European Centre for Disease Prevention and Control (2020). "Personal Protective Equipment (PPE) Needs in Healthcare Settings for the Care of Patients with Suspected or Confirmed Novel Coronavirus (2019- nCoV)". Online. www.ecdc.europa.eu/sites/default/files/documents/novel-coronavirus-personal-protective-equipment-needs-healthcare-settings.pdf.

Facher, Lev (Mar. 2020). "The Coronavirus Outbreak has Left Medical Supplies in Short Supply. Is the Nation's Emergency Stockpile Ready to Help?" *STAT*. Online. www.statnews.com/2020/03/10/coronavirus-strategic-national-stockpile/.

Feng, Runhuan, and Jose Garrido (2011). “Actuarial Applications of Epidemiological Models”. In: *North American Actuarial Journal* 15.1, pp. 112–136.

Fernández-Villaverde, Jesús, and Charles I. Jones (May 2020). *Estimating and Simulating a SIRD Model of COVID-19 for Many Countries, States, and Cities*. Working Paper 27128. National Bureau of Economic Research.

Fu, Anqi, Balasubramanian Narasimhan, and Stephen Boyd (2020). “CVXR: An R Package for Disciplined Convex Optimization”. In: *Journal of Statistical Software* 94.14.

Giordano, Giulia, Franco Blanchini, Raffaele Bruno, Patrizio Colaneri, Alessandro Di Filippo, Angela Di Matteo, and Marta Colaneri (June 1, 2020). “Modelling the COVID-19 Epidemic and Implementation of Population-wide Interventions in Italy”. In: *Nature Medicine* 26.6, pp. 855–860.

Grant, Michael, Stephen Boyd, and Yinyu Ye (2006). “Disciplined Convex Programming”. In: *Global Optimization: From Theory to Implementation*. Ed. by Leo Liberti and Nelson Maculan. Springer. Chap. 7, pp. 155–210.

Grasselli, Giacomo, Alberto Zangrillo, Alberto Zanella, Massimo Antonelli, Luca Cabrini, Antonio Castelli, Danilo Cereda, Antonio Coluccello, Giuseppe Foti, Roberto Fumagalli, Giorgio Iotti, Nicola Latronico, Luca Lorini, Stefano Merler, Giuseppe Natalini, Alessandra Piatti, Marco Vito Ranieri, Anna Mara Scandroglio, Enrico Storti, Maurizio Cecconi, and Antonio Pesenti (Apr. 2020). “Baseline Characteristics and Outcomes of 1591 Patients Infected With SARS-CoV-2 Admitted to ICUs of the Lombardy Region, Italy”. In: *JAMA* 323.16, pp. 1574–1581.

Greer, Amy L., and Dena Schanzer (June 2013). “Using a Dynamic Model to Consider Optimal Antiviral Stockpile Size in the Face of Pandemic Influenza Uncertainty”. In: *PLoS ONE* 8.6. Ed. by Man-Seong Park, e67253.

Gregory, Victoria, Guido Menzio, and David G. Wiczer (May 2020). *Pandemic Recession: L or V-Shaped?* Working Paper 27105. National Bureau of Economic Research.

Hill, Alison, Mike Levy, Sherrie Xie, Justin Sheen, Julianna Shinnick, Andrei Gheorghe, and Chris Rehmann (Mar. 2020). *Modeling COVID-19 Spread vs Healthcare Capacity*. Online. https://alhill.shinyapps.io/COVID19seir/.

Hillairet, Caroline, and Olivier Lopez (2021). “Propagation of Cyber Incidents in an Insurance Portfolio: Counting Processes Combined with Compartmental Epidemiological Models”. In: *Scandinavian Actuarial Journal*, DOI: 10.1080/03461238.2021.1872694.

Holdren, John P., Christine Cassel, Chris Chyba, Susan Graham, Eric Lander, Ed Penhoet, William Press, Maxine Savitz, and Harold Varmus (2020). “Recommendations for the National Strategic Pandemic Stockpile”. Belfer Center. Online. www.belfercenter.org/publication/recommendations-national-strategic-pandemic-stockpile.

Holveck, Brandon, Dustin Racioppi, and Alexis Shanes (2020). “Delaware Partners with Northeast States to Buy PPE, Medical Supplies”. *Delaware Online*. Online. www.delawareonline.com/story/news/coronavirus-in-delaware/2020/05/03/nj-ny-de-pa-ct-northeast-states-form-regional-supply-chain-ppe/3074768001/.

Hortaçsu, Ali, Jiarui Liu, and Timothy Schwieg (Jan. 2021). “Estimating the Fraction of Unreported Infections in Epidemics with a Known Epicenter: An Application to COVID-19”. In: *Journal of Econometrics* 220.1, pp. 106–129.

Hua, Chen, and Samual H. Cox (2009). “An Option-Based Operational Risk Management Model for Pandemics”. In: *North American Actuarial Journal* 13.1, pp. 54–76.

International Monetary Fund (Jan. 1, 2021). *World Economic Outlook Update: Policy Support and Vaccines Expected to Lift Activity*. Online. www.imf.org/en/Publications/WEO/Issues/2021/01/26/2021-world-economic-outlook-update.

Jamison, Dean T., Hellen Gelband, Susan Horton, Prabhat Jha, Ramanan Laxminarayan, Charles N. Mock, and Rachel Nugent (Nov. 2017). *Disease Control Priorities, Third Edition (Volume 9): Improving Health and Reducing Poverty*. Washington, DC: World Bank.

Jones, Kate E., Nikkita G. Patel, Marc A. Levy, Adam Storeygard, Deborah Balk, John L. Gittleman, and Peter Daszak (Feb. 2008). “Global Trends in Emerging Infectious Diseases”. In: *Nature* 451.7181, pp. 990–993.

Lefèvre, Claude, and Philippe Picard (2018). “Final Outcomes and Disease Insurance for a Controlled Epidemic Model”. In: *Appl. Stoch. Models Bus. Ind*. 34.6, pp. 803–815.

Lefèvre, Claude, Philippe Picard, and Matthieu Simon (2017). “Epidemic Risk and Insurance Coverage”. In: *J. Appl. Probab.* 54.1, pp. 286–303.

Lefèvre, Claude, and Matthieu Simon (2020). “SIR-type Epidemic Models as Block-structured Markov Processes”. In: *Methodol. Comput. Appl. Probab*. 22.2, pp. 433–453.

Leung, Kathy, Joseph T. Wu, Di Liu, and Gabriel M. Leung (Apr. 2020). “First-wave COVID-19 Transmissibility and Severity in China Outside Hubei after Control Measures, and Second-wave Scenario Planning: A Modelling Impact assessment”. In: *The Lancet* 395.10233, pp. 1382–1393.

Morse, Stephen S. (Mar. 1995). “Factors in the Emergence of Infectious Diseases”. In: *Emerging Infectious Diseases* 1.1, pp. 7–15.

Patel, Nisarg A. (Mar. 2020). “America Needs More Ventilators. Here’s How We Can Get Them”. *Slate*. Online. https://slate.com/technology/2020/03/how-america-could-get-the-ventilators-it-needs.html.

Porpora, Tracey (Mar. 2020). “What Is a Ventilator? How Much Does One Cost?” *SIlive*. Online. www.silive.com/coronavirus/2020/03/what-is-a-ventilator-how-much-does-one-cost.html.

Preidt, Robert (Apr. 2020). “Most COVID-19 Patients Placed on Ventilators Died, New York Study Shows”. *US News*. Online. www.usnews.com/news/health-news/articles/2020-04-22/most-covid-19-patients-placed-on-ventilators-died-new-york-study-shows.

Ranney, Megan L., Valerie Griffeth, and Ashish K. Jha (Apr. 2020). “Critical Supply Shortages: The Need for Ventilators and Personal Protective Equipment during the Covid-19 Pandemic”. In: *New England Journal of Medicine* 382.18, e41.

Rosenbaum, Lisa (May 2020). “Facing Covid-19 in Italy: Ethics, Logistics, and Therapeutics on the Epidemic’s Front Line”. In: *New England Journal of Medicine* 382.20, pp. 1873–1875.

Rowland, Christopher (Mar. 2020). “More Lifesaving Ventilators Are Available. Hospitals Can’t Afford Them”. *Washington Post*. Online. www.washingtonpost.com/health/2020/03/18/ventilator-shortage-hospital-icu-coronavirus/.

Segal, Sim (Apr. 5, 2011). *Corporate Value of Enterprise Risk Management*. Hoboken, NJ: John Wiley & Sons.

Siddiqui, M. Ruby, and W. John Edmunds (Feb. 2008). “Cost-effectiveness of Antiviral Stockpiling and Near-Patient Testing for Potential Influenza Pandemic”. In: *Emerging Infectious Diseases* 14.2, pp. 267– 274.

Stauffer, Jon M., and Subodha Kumar (2021). “Impact of Incorporating Returns into Pre-Disaster Deployments for Rapid-Onset Predictable Disasters”. In: *Production and Operations Management* 30.2, pp. 451– 474.

The Atlantic (May 2020). “The COVID Tracking Project”. Online. https://covidtracking.com/api.

Tian, Huaiyu, Yonghong Liu, Yidan Li, Chieh-Hsi Wu, Bin Chen, Moritz U. G. Kraemer, Bingying Li, Jun Cai, Bo Xu, Qiqi Yang, Ben Wang, Peng Yang, Yujun Cui, Yimeng Song, Pai Zheng, Quanyi Wang, Ottar N. Bjornstad, Ruifu Yang, Bryan T. Grenfell, Oliver G. Pybus, and Christopher Dye (Mar. 2020). “An Investigation of Transmission Control Measures during the First 50 Days of the COVID-19 Epidemic in China”. In: *Science* 368.6491, pp. 638–642.

Tobin-Tyler, Elizabeth (2020). “In Allocating Scarce Health Care Resources During COVID-19, Don’t Forget Health Justice”. *Health Affairs Blog*, DOI: 10.1377/hblog20200422.50144.

US Centers for Disease Control and Prevention (2012). “Principles of Epidemiology in Public Health Practice.” Online. www.cdc.gov/csels/dsepd/ss1978/lesson1/section11.html

US Centers for Disease Control and Prevention (2018). “Tularemia”. Online. www.cdc.gov/tularemia/index.html

Vanajakumari, Manoj, Subodha Kumar, and Sushil Gupta (Feb. 2016). “An Integrated Logistic Model for Predictable Disasters”. In: *Production and Operations Management* 25.5, pp. 791–811.

World Health Organization (2018). “Rift Valley Fever”. Online. www.who.int/news-room/fact-sheets/detail/rift-valley-fever

World Health Organization (2019). “Japanese Encephalitis”. Online. www.who.int/news-room/fact-sheets/detail/japanese-encephalitis

Worldometer (2021). “Coronavirus Cases”. Online. www.worldometers.info/coronavirus/.

Wu, Zunyou, and Jennifer M. McGoogan (Apr. 2020). “Characteristics of and Important Lessons From the Coronavirus Disease 2019 (COVID-19) Outbreak in China”. In: *JAMA* 323.13, p. 1239.

Yang, Penghui, Yibo Ding, Zhe Xu, Rui Pu, Ping Li, Jin Yan, Jiluo Liu, Fanping Meng, Lei Huang, Lei Shi, Tianjun Jiang, Enqiang Qin, Min Zhao, Dawei Zhang, Peng Zhao, Lingxiang Yu, Zhaohai Wang, Zhixian Hong, Zhaohui Xiao, Qing Xi, Dexi Zhao, Peng Yu, Caizhong Zhu, Zhu Chen, Shaogeng Zhang, Junsheng Ji, Guangwen Cao, and Fusheng Wang (2020). “Epidemiological and Clinical

Features of COVID-19 Patients with and without Pneumonia in Beijing, China". In: *medRxiv*, DOI: https://doi.org/10.1101/2020.02.28.20028068.

Yang, Xiaobo, Yuan Yu, Jiqian Xu, Huaqing Shu, Jia'an Xia, Hong Liu, Yongran Wu, Lu Zhang, Zhui Yu, Minghao Fang, Ting Yu, Yaxin Wang, Shangwen Pan, Xiaojing Zou, Shiying Yuan, and You Shang (May 2020). "Clinical Course and Outcomes of Critically Ill Patients with SARS-CoV-2 Pneumonia in Wuhan, China: A Single-centered, Retrospective, Observational Study". In: *The Lancet Respiratory Medicine* 8.5, pp. 475–481.

Appendix A: Analytical Solutions and Proofs

A.1 Stockpiling of durable resources

The optimization problem for the stockpiling of durable resources is as follows:

$$\min_{K_0 \geq 0} \sum_{j=1}^{m} \omega_j \left(\frac{\theta_j^+}{2} (X_j - (K_0 + aj))_+^2 + \frac{\theta_j^-}{2} (X_j - (K_0 + aj))_-^2 + c_j (K_0 + aj) \right) + c_0 K_0.$$

Theorem A.1. *Let* $Y_j = X_j - aj$, $\forall j = 1, 2, \cdots, m$. *Let* $S = \sum^{m} \omega_j c_j + c_0$. *Let* $Y_{[1]} \leq Y_{[2]} \leq \cdots \leq Y_{[m]}$ *be the increasingly ordered sequence of* $Y_1, Y_2, \cdots, Y_m$. *Let* $J = 1, 2, \cdots, m$ *such that*

$$\sum_{j=1}^{J-1} \omega_{[j]} \theta_{[j]}^- (Y_{[j]} - Y_{[J]}) + \sum_{j=J}^{m} \omega_{[j]} \theta_{[j]}^+ (Y_{[j]} - Y_{[J]}) \leq S \leq \sum_{j=1}^{J-1} \omega_{[j]} \theta_{[j]}^- (Y_{[j]} - Y_{[J-1]}) + \sum_{j=J}^{m} \omega_{[j]} \theta_{[j]}^+ (Y_{[j]} - Y_{[J-1]}),$$

where we define that when $J = 1$,

$$\sum_{j=1}^{J-1} \omega_{[j]} \theta_{[j]}^- (Y_{[j]} - Y_{[J]}) + \sum_{j=J}^{m} \omega_{[j]} \theta_{[j]}^+ (Y_{[j]} - Y_{[J]}) = \sum_{j=1}^{m} \omega_{[j]} \theta_{[j]}^+ (Y_{[j]} - Y_{[1]}),$$

$$\sum_{j=1}^{J-1} \omega_{[j]} \theta_{[j]}^- (Y_{[j]} - Y_{[J-1]}) + \sum_{j=J}^{m} \omega_{[j]} \theta_{[j]}^+ (Y_{[j]} - Y_{[J-1]}) = \infty.$$

Let

$$K_0' = \frac{\sum_{j=1}^{J-1} \omega_{(j)} \theta_{(j)}^- Y_{(j)} + \sum_{j=J}^{m} \omega_{(j)} \theta_{(j)}^+ Y_{(j)} - S}{\sum_{j=1}^{J-1} \omega_{(j)} \theta_{(j)}^- + \sum_{j=J}^{m} \omega_{(j)} \theta_{(j)}^+}.$$

If $K_0 < 0$, then the optimal initial stockpile (which minimizes the objective function above) $K_0^* = 0$, and if $K_0 \geq 0$, then $K_0^* = K_0$.

Proof. Let $Y_j = X_j - aj$, $\forall j = 1, 2, \cdots, m$. Let $Y_{[1]} \leq Y_{[2]} \leq \cdots \leq Y_{[m]}$ be the increasingly ordered sequence of $Y_1, Y_2, \cdots, Y_m$. In that case, Y_j represents the daily shortage when the initial stockpile is completely missing. Then the objective function becomes

$$F(K_0) := \sum_{j=1}^{m} \omega_{[j]} \left(\frac{\theta_{[j]}^+}{2} (Y_{[j]} - K_0)_+^2 + \frac{\theta_{[j]}^-}{2} (K_0 - Y_{[j]})_+^2 \right) + \left(\sum_{j=1}^{m} \omega_j c_j + c_0 \right) K_0 + \sum_{j=1}^{m} \omega_j c_j a j.$$

Note that $F(K_0)$ is a convex function in K_0 for any $K_0 \in \mathrm{R}$. Let

$$G(K_0) = \sum_{j=1}^{m} \omega_{[j]} \left(\frac{\theta_{[j]}^+}{2} (Y_{[j]} - K_0)_+^2 + \frac{\theta_{[j]}^-}{2} (K_0 - Y_{[j]})_+^2 \right),$$

$$S = \sum_{j=1}^{m} \omega_j c_j + c_0,$$

where $G(\cdot)$ is convex in K_0.

The first-order derivatives of G at $Y_{[1]}$ and $Y_{[m]}$ are as follows:

$$G'(Y_{[1]}) = \sum_{j=1}^{m} \omega_{[j]} \theta^{-}_{[j]} (Y_{[1]} - Y_{[j]}) \leq 0.$$

$$G'(Y_{[m]}) = \sum_{j=1}^{m} \omega_{[j]} \theta^{+}_{[j]} (Y_{[j]} - Y_{[m]})(-1) = \sum_{j=1}^{m} \omega_{[j]} \theta^{+}_{[j]} (Y_{[m]} - Y_{[j]}) \geq 0.$$

Then $\exists\, \tilde{K}_0 \in [Y_{[1]}, Y_{[m]}]$ such that $G'(\tilde{K}_0) = 0$. Since $S = \sum_{j=1}^{m} \omega_j c_j + c_0 \geq 0, \exists K_0' \in (-\infty, Y_{[m]}]$ such that $_{0[m]} F(K_0) = 0$, i.e., $\exists\, J = 1, \cdots, m$ such that $K_0' \in [Y_{[J-1]}, Y_{[J]}]$, where we define $Y_{(0)} = -\infty$, and $F'(K_0') = 0$.

Here, we are relaxing the constraint that the initial stockpile has to be non-negative, but we will add it back in the end. The key observation is that given all the $(Y_{[j]})_{j \in \{0,\ldots,m\}}$, we can always find a K_0 between two adjacent $Y_{[j]}$'s, $Y_{[J-1]}$ and $Y_{[J]}$, that minimize the objective function. That is,

$$F'(K_0') = \sum_{j=1}^{J-1} \omega_{[j]} \theta^{-}_{[j]} (K_0' - Y_{[J]}) + \sum_{j=J}^{m} \omega_{[j]} \theta^{+}_{[j]} (Y_{[j]} - K_0')(-1) + S = 0.$$

Then

$$K_0' = \frac{\sum_{j=1}^{J-1} \omega_{[j]} \theta^{-}_{[j]} Y_{[j]} + \sum_{j=J}^{m} \omega_{[j]} \theta^{+}_{[j]} Y_{[j]} - S}{\sum_{j=1}^{J-1} \omega_{[j]} \theta^{-}_{[j]} + \sum_{j=J}^{m} \omega_{[j]} \theta^{+}_{[j]}}.$$

Therefore, the condition that $K_0' \in [Y_{[J-1]}, Y_{[J]}]$ is given by

$$Y_{[J-1]} \leq \frac{\sum_{j=1}^{J-1} \omega_{[j]} \theta^{-}_{[j]} Y_{[j]} + \sum_{j=J}^{m} \omega_{[j]} \theta^{+}_{[j]} Y_{[j]} - S}{\sum_{j=1}^{J-1} \omega_{[j]} \theta^{-}_{[j]} + \sum_{j=J}^{m} \omega_{[j]} \theta^{+}_{[j]}} \leq Y_{[J]}.$$

Or equivalently, $\exists\, J = 1, 2, \ldots, m$, such that

$$\sum_{j=1}^{J-1} \omega_{[j]} \theta^{-}_{[j]} (Y_{[j]} - Y_{[J]}) + \sum_{j=J}^{m} \omega_{[j]} \theta^{+}_{[j]} (Y_{[j]} - Y_{[J]}) \leq S \leq \sum_{j=1}^{J-1} \omega_{[j]} \theta^{-}_{[j]} (Y_{[j]} - Y_{[J-1]}) + \sum_{j=J}^{m} \omega_{[j]} \theta^{+}_{[j]} (Y_{[j]} - Y_{[J-1]}),$$

wherein if $J = 1$, we define

$$\sum_{j=1}^{J-1} \omega_{[j]} \theta^{-}_{[j]} (Y_{[j]} - Y_{[J]}) + \sum_{j=J}^{m} \omega_{[j]} \theta^{+}_{[j]} (Y_{[j]} - Y_{[J]}) = \sum_{j=1}^{m} \omega_{[j]} \theta^{+}_{[j]} (Y_{[j]} - Y_{[1]}),$$

$$\sum_{j=1}^{J-1} \omega_{[j]} \theta^{-}_{[j]} (Y_{[j]} - Y_{[J-1]}) + \sum_{j=J}^{m} \omega_{[j]} \theta^{+}_{[j]} (Y_{[j]} - Y_{[J-1]}) = \infty.$$

Finally, given the non-negativity of the stockpile, if $K_0 < 0$, then the optimal initial stockpile $K_0^* = 0$, and if $K_0 \geq 0$, then $K_0^* = K_0$.

A.2 Centralized resources allocation

The optimization problem for allocating resources amount regions is as follows:

$$\min_{\substack{K_j^{(i)}\geq 0; i=1,2,\ldots,n; \\ j=1,2,\ldots,m}} \sum_{j=1}^{m}\sum_{i=1}^{n}\omega_j^{(i)}\left(\frac{\theta_j^{+(i)}}{2}\left(X_j^{(i)}-K_j^{(i)}\right)_+^2+\frac{\theta_j^{-(i)}}{2}\left(X_j^{(i)}-K_j^{(i)}\right)_-^2\right)$$

$$\text{such that } \sum_{i=1}^{n}K_j^{(i)}=K_j, \quad \text{for } j=1,2,\ldots,m,$$

Theorem A.2. *The optimization above is done from period to period, and thus to simplify notation, the time indicator j can be dropped at each time point. Let* $X^{[1]}\geq\ldots\geq X^{[n]}>0$ *be the decreasingly ordered sequence of* $X^{(1)}, X^{(2)}, \ldots, X^{(n)}$.

If $K>\sum_{r=1}^{n}X^{(r)}=X$, *then*

$$K^{(i)}=\left(1-\frac{\frac{1}{\omega^{(i)}\theta^{-(i)}}}{\sum_{r=1}^{n}\frac{1}{\omega^{(r)}\theta^{-(r)}}}\right)X^{(i)}+\frac{\frac{1}{\omega^{(i)}\theta^{-(i)}}}{\sum_{r=1}^{n}\frac{1}{\omega^{(r)}\theta^{-(r)}}}\left(K-\sum_{r\neq i}X^{(r)}\right),\forall i=1,2,\ldots,n.$$

If $K\leq\sum_{r=1}^{n}X^{(r)}=X$, *we can find an* $I=1,2,\ldots,n$ *such that* $K\leq\sum_{r=1}^{I}X^{[r]}$,

$$X^{[i]}\geq\frac{\frac{1}{\omega^{[i]}\theta^{+[i]}}}{\sum_{r=1}^{I}\frac{1}{\omega^{[r]}\theta^{+[r]}}}\left(\sum_{r=1}^{I}X^{[r]}-K\right),\forall i=1,\ldots,I,$$

$$X^{[i]}<\frac{\frac{1}{\omega^{[i]}\theta^{+[i]}}}{\sum_{r=1}^{I}\frac{1}{\omega^{[r]}\theta^{+[r]}}}\left(\sum_{r=1}^{I}X^{[r]}-K\right),\forall i=I+1,I+2,\ldots,n.$$

Then $K^{[I+1]}=\cdots=K^{[n]}=0$.

$$K^{[i]}=\left(1-\frac{\frac{1}{\omega^{[i]}\theta^{+[i]}}}{\sum_{r=1}^{I}\frac{1}{\omega^{[r]}\theta^{+[r]}}}\right)X^{[i]}+\frac{\frac{1}{\omega^{[i]}\theta^{+[i]}}}{\sum_{r=1}^{I}\frac{1}{\omega^{[r]}\theta^{+[r]}}}\left(K-\sum_{r=1,r\neq i}^{I}X^{[r]}\right),\forall i=1,\ldots,I.$$

Proof. At each time point *j*, we want to solve the following optimization problem,

$$\min_{K^{(i)};i=1,2,\cdots,n}\sum_{i=1}^{n}\omega^{(i)}\left(\frac{\theta^{+(i)}}{2}(X^{(i)}-K^{(i)})_+^2+\frac{\theta^{-(i)}}{2}(K^{(i)}-X^{(i)})_+^2\right)$$

$$\text{such that } \sum_{i=1}^{n}K^{(i)}=K, K^{(i)}\geq 0, \forall i=1,2,\cdots,n.$$

Case 1: Coexisting surpluses and shortages

First, let us consider the case in which some regions are having surpluses, whereas other regions are experiencing shortages at the same time. We shall show below that this case is impossible regardless of the non-negative constraints. That is, suppose that $K^{(1)}$, $K^{(2)}$, ..., $K^{(n)}$ lie locally in a feasible set, such that I of them satisfy $K^{(i)} > X^{(i)}$, where $I = 1, 2, ..., n-1$. The remaining $n - I$ of them satisfy $K^{(i)} \leq X^{(i)}$. Without loss of generality, assume the first I of $K^{(i)}$ are in the former group. Then the local problem becomes

$$\min_{K^{(i)};i=1,2,\cdots,n} \sum_{i=I+1}^{n} \omega^{(i)} \frac{\theta^{+(i)}}{2} (X^{(i)} - K^{(i)})^2 + \sum_{i=1}^{I} \omega^{(i)} \frac{\theta^{-(i)}}{2} (X^{(i)} - K^{(i)})^2$$

such that $$\sum_{i=1}^{n} K^{(i)} = K.$$

The solution to this problem is given by

$$K^{(i)} = \left(1 - \frac{\frac{1}{\omega^{(i)}\theta^{-(i)}}}{\sum_{r=1}^{I} \frac{1}{\omega^{(r)}\theta^{-(r)}} + \sum_{r=I+1}^{n} \frac{1}{\omega^{(r)}\theta^{+(r)}}}\right) X^{(i)} + \frac{\frac{1}{\omega^{(i)}\theta^{-(i)}}}{\sum_{r=1}^{I} \frac{1}{\omega^{(r)}\theta^{-(r)}} + \sum_{r=I+1}^{n} \frac{1}{\omega^{(r)}\theta^{+(r)}}} \left(K - \sum_{r \neq i} X^{(r)}\right),$$

for $i = 1, 2, ..., I$, and

$$K^{(i)} = \left(1 - \frac{\frac{1}{\omega^{(i)}\theta^{+(i)}}}{\sum_{r=1}^{I} \frac{1}{\omega^{(r)}\theta^{-(r)}} + \sum_{r=I+1}^{n} \frac{1}{\omega^{(r)}\theta^{+(r)}}}\right) X^{(i)} + \frac{\frac{1}{\omega^{(i)}\theta^{+(i)}}}{\sum_{r=1}^{I} \frac{1}{\omega^{(r)}\theta^{-(r)}} + \sum_{r=I+1}^{n} \frac{1}{\omega^{(r)}\theta^{+(r)}}} \left(K - \sum_{r \neq i} X^{(r)}\right),$$

for $i = I + 1, ..., n$.

However, $\forall i = 1, 2 \ldots, I,\ K^{(i)} > X^{(i)}$, and $\forall i = I+1, \ldots, n,\ K^{(i)} \leq X^{(i)}$, which implies $K > \sum_{r=1}^{n} X^{(r)}$ and $K \leq \sum_{r=1}^{n} X^{(r)}$, and thus we have a contradiction. This result shows that it is impossible for some regions to have surpluses while other regions are experiencing shortages. Therefore, it suffices to only consider the scenarios that there is a system-wide surplus and that there is a system-wide shortage.

Case 2: System-wide surplus

If there is a system-wide surplus – i.e., all regions have surpluses – then the problem becomes

$$\min_{K^{(i)};i=1,2,\cdots,n} \sum_{i=1}^{n} \omega^{(i)} \frac{\theta^{-(i)}}{2} (K^{(i)} - X^{(i)})^2$$

$$\sum_{i=1}^{n} K^{(i)} = K,$$

such that $K^{(i)} > X^{(i)}, \forall i = 1, \ldots, n.$

The solution is given by

$$K^{(i)} = \left(1 - \frac{\frac{1}{\omega^{(i)}\theta^{-(i)}}}{\sum_{r=1}^{n}\frac{1}{\omega^{(r)}\theta^{-(r)}}}\right)X^{(i)} + \frac{\frac{1}{\omega^{(i)}\theta^{-(i)}}}{\sum_{r=1}^{n}\frac{1}{\omega^{(r)}\theta^{-(r)}}}\left(K - \sum_{r\neq i} X^{(r)}\right).$$

For this result to hold, we only need the condition that $K > \sum_{r=1}^{n} X^{(r)} = X$. Due to uniqueness, under this condition, this $K^{(i)}$ is optimal.

Case 3: System-wide shortage

It remains to solve the case that there is a system-wide shortage; i.e., all regions have shortages. In that case, the problem becomes

$$\min_{K^{(i)};i=1,2,\cdots,n} \sum_{i=1}^{n} \omega^{(i)} \frac{\theta^{+(i)}}{2}(X^{(i)} - K^{(i)})^2$$

$$\sum_{i=1}^{n} K^{(i)} = K;$$

such that $0 \leq K^{(i)} \leq X^{(i)}, \forall i = 1, \cdots, n.$

Apart from the given condition that $\sum_{i=1}^{n} K^{(i)} = K$, there are additional inequality constraints in this optimization problem. Hence, we make use of Karush–Kuhn–Tucker (KKT) conditions as follows:

$$\begin{aligned}
&\omega^{(i)}\theta^{+(i)}(K^{(i)} - X^{(i)}) - \lambda_1^{(i)} + \lambda_2^{(i)} + \mu = 0,\\
&0 \leq K^{(i)} \leq X^{(i)},\\
&\lambda_1^{(i)} \geq 0, \quad \lambda_1^{(i)}K^{(i)} = 0,\\
&\lambda_2^{(i)} \geq 0, \quad \lambda_2^{(i)}(K^{(i)} - X^{(i)}) = 0,
\end{aligned}$$

for all i = 1, …, n. Regarding the values of $\lambda^{(i)}$ and $\lambda^{(i)}$, we can consider the following four mutually exclusive cases,

1. $\lambda_1^{(i)} > 0$ for some $i = 1, \cdots, n,$ and $\lambda_2^{(i)} > 0$ for some $i = 1, \cdots, n$;
2. $\lambda_1^{(i)} = 0$ for all $i = 1, \cdots, n,$ and $\lambda_2^{(i)} > 0$ for some $i = 1, \cdots, n$;
3. $\lambda_1^{(i)} = 0$ for some $i = 1, \cdots, n,$ and $\lambda_2^{(i)} = 0$ for all $i = 1, \cdots, n$;
4. $\lambda_1^{(i)} = 0$ for all $i = 1, \cdots, n,$ and $\lambda_2^{(i)} = 0$ for all $i = 1, \cdots, n$.

Each of them will be discussed as follows.

Case 3.1: $\lambda_1^{(i)} > 0$ for some $i = 1, \cdots, n,$ and $\lambda_2^{(i)} > 0$ for some $i = 1, \cdots, n$.

We will show that this case will lead to a contradiction, and thus is impossible. Because the ordering of $\lambda_1^{(i)}$ and $\lambda_2^{(i)}$ does not affect the conditions, for simplicity we rearrange them in such a way that there is an $I = 1, 2, \ldots, n-1$, and an $\tilde{I} = 1, 2, \ldots, n-1$, for which

$$\begin{aligned}
\lambda_1^{[i]} &> 0, \quad \forall i = 1, \ldots, I, \\
\lambda_1^{[i]} &= 0, \quad \forall i = I+1, \ldots, n, \\
\lambda_2^{[i]} &= 0, \quad \forall i = 1, \ldots, n-\tilde{I}, \\
\lambda_2^{[i]} &> 0, \quad \forall i = n-\tilde{I}+1, \ldots, n,
\end{aligned}$$

where [*i*] are indices after the rearrangement.

We also have the condition that $I \leq n - \tilde{I}$, because for each i, $\lambda_1^{[i]} > 0$ implies $K^{[i]} = 0$, which further implies $\lambda_2^{[i]} = 0$. Therefore, the number of $\lambda_2^{[i]}$ that are equal to 0 (i.e., $n - \tilde{I}$) is at least the number of $\lambda_1^{[i]}$ that are greater than 0; i.e., I. Then by the complementary slackness conditions in the KKT conditions above, $K^{[i]} = 0, \forall i = 1, 2, \cdots, I$ and $K^{[i]} = X^{[i]}, \forall i = n - \tilde{I} + 1, \cdots, n$.

Then, the KKT conditions are simplified.

$$\begin{aligned}
-\omega^{[i]}\theta^{+[i]}X^{[i]} - \lambda_1^{[i]} + \mu &= 0, \quad \forall i = 1, \ldots, I \\
\omega^{[i]}\theta^{+[i]}(K^{[i]} - X^{[i]}) + \mu &= 0, \quad \forall i = I+1, \ldots, n-\tilde{I} \\
\lambda_2^{[i]} + \mu &= 0, \quad \forall i = n-\tilde{I}+1, \ldots, n \\
0 \leq K^{[i]} &\leq X^{[i]}, \quad \forall i = I+1, \ldots, n-\tilde{I}
\end{aligned}$$

$$\sum_{r=I+1}^{n-\tilde{I}} K^{[r]} = K - \sum_{r=n-\tilde{I}+1}^{n} X^{[r]},$$

from which we can observe the following contradiction that

$$\begin{aligned}
\mu &= -\lambda_2^{[n]} < 0 \\
\mu &= \omega^{[1]}\theta^{+[1]}X^{[1]} + \lambda_1^{[1]} > 0.
\end{aligned}$$

Therefore, we can conclude that if $\tilde{I} = 1, \cdots, n-1,$, then $I = 0$ or n, and its contrapositive is also true, which states that if $I = 1, \cdots, n-1,$ then $\tilde{I} = 0$ or n. These two statements correspond with the second and third cases respectively, and they are considered as follows.

Case 3.2: $\lambda_1^{(i)} = 0$ for all $i = 1, \cdots, n,$, and $\lambda_2^{(i)} > 0$ for some $i = 1, \cdots, n$.

As in the previous case, We use the rearranged $\lambda_1^{[i]}$ and $\lambda_2^{[i]}$, so now $\lambda_2^{[i]} = 0$, for all $i = 1, \ldots, n - \tilde{I}$, and $\lambda_2^{[i]} > 0$, for all $i = n - \tilde{I} + 1, \ldots, n$, for some $\tilde{I} = 1, 2, \ldots, n - 1$. This implies $K^{[i]} = X^{[i]}$, for all $i = n - \tilde{I} + 1, \ldots, n$.

In this case, the KKT conditions become

$$\begin{aligned} \omega^{[i]}\theta^{+[i]}(K^{[i]} - X^{[i]}) + \mu = 0, \quad & \forall i = 1, \ldots, n - \tilde{I} \\ \lambda_2^{[i]} + \mu = 0, \quad & \forall i = n - \tilde{I} + 1, \ldots, n \\ 0 \le K^{[i]} \le X^{[i]}, \quad & \forall i = 1, \cdots, n - \tilde{I} \\ \sum_{r=1}^{n-\tilde{I}} K^{(r)} = K - \sum_{r=n-\tilde{I}+1}^{n} X^{(r)}. & \end{aligned}$$

By solving this system, we get

$$\begin{aligned} K^{[i]} &= \left(1 - \frac{\frac{1}{\omega^{[i]}\theta^{+[i]}}}{\sum_{r=1}^{n-\tilde{I}} \frac{1}{\omega^{[r]}\theta^{+[r]}}}\right) X^{[i]} + \frac{\frac{1}{\omega^{[i]}\theta^{+[i]}}}{\sum_{r=1}^{n-\tilde{I}} \frac{1}{\omega^{[r]}\theta^{+[r]}}} \left(K - \sum_{r \neq i}^{n} X^{[r]}\right) \\ &= X^{[i]} + \frac{\frac{1}{\omega^{[i]}\theta^{+[i]}}}{\sum_{r=1}^{n-\tilde{I}} \frac{1}{\omega^{[r]}\theta^{+[r]}}} \left(K - \sum_{r=1}^{n} X^{[r]}\right), \quad \forall i = 1, 2, \cdots, n - \tilde{I} \\ \mu &= \frac{1}{\sum_{r=1}^{n-\tilde{I}} \frac{1}{\omega^{[r]}\theta^{+[r]}}} \left(\sum_{r=1}^{n} X^{[r]} - K\right) \\ \lambda_2^{[i]} &= -\mu = -\frac{1}{\sum_{r=1}^{n-\tilde{I}} \frac{1}{\omega^{[r]}\theta^{+[r]}}} \left(\sum_{r=1}^{n} X^{[r]} - K\right), \quad \forall i = n - \tilde{I} + 1, \cdots, n. \end{aligned}$$

By the system-wide shortage assumption, $\sum_{r=1}^{n} X^{[r]} - K \ge 0$, and therefore, $\lambda_2^{[i]} \le 0$ for all $i = n - \tilde{I} + 1, \cdots, n$. But this contradicts the assumption that $\lambda_2^{[i]} > 0$ for all $i = n - \tilde{I} + 1, \cdots, n$. Therefore, we can tell that this is another impossible case.

Case 3.3: $\lambda_1^{(i)} > 0$ for some $i = 1, \cdots, n$, and $\lambda_2^{(i)} = 0$ for all $i = 1, \cdots, n$.

Again, for this case, we use the rearranged $\lambda_1^{[i]}$ and $\lambda_2^{[i]}$ for $i = 1, \ldots, n$. And we assume that there is an $I = 1, 2, \ldots, n - 1$, such that $\lambda_1^{[i]} > 0$ for $i = 1, \ldots, I$, and $\lambda_1^{[i]} = 0$ for $i = I + 1, \ldots, n$. This implies $i = 1, \ldots, I$, and we get the following conditions:

$$
\begin{aligned}
-\omega^{[i]}\theta^{+[i]}X^{[i]} - \lambda_1^{[i]} + \mu = 0, \quad & \forall i = 1, \ldots, I \\
\omega^{[i]}\theta^{+[i]}(K^{[i]} - X^{[i]}) + \mu = 0, \quad & \forall i = I+1, \ldots, n \\
0 \le K^{[i]} \le X^{[i]}, \quad & \forall i = I+1, \cdots, n \\
\sum_{i=I+1}^{n} X^{[r]} = K.
\end{aligned}
$$

They together give us

$$
\begin{aligned}
K^{[i]} &= \left(1 - \frac{\frac{1}{\omega^{[i]}\theta^{+[i]}}}{\sum_{r=I+1}^{n} \frac{1}{\omega^{[r]}\theta^{+[r]}}}\right) X^{[i]} + \frac{\frac{1}{\omega^{[i]}\theta^{+[i]}}}{\sum_{r=I+1}^{n} \frac{1}{\omega^{[r]}\theta^{+[r]}}} \left(K - \sum_{r=I+1}^{n} X^{[r]}\right) \\
&= X^{[i]} + \frac{\frac{1}{\omega^{[i]}\theta^{+[i]}}}{\sum_{r=I+1}^{n} \frac{1}{\omega^{[r]}\theta^{+[r]}}} \left(K - \sum_{r=I+1}^{n} X^{[r]}\right), \quad \forall i = I+1, \cdots, n. \\
\mu &= \frac{1}{\sum_{r=I+1}^{n} \frac{1}{\omega^{[r]}\theta^{+[r]}}} \left(\sum_{r=I+1}^{n} X^{[r]} - K\right) \\
\lambda_1^{[i]} &= \frac{1}{\sum_{r=I+1}^{n} \frac{1}{\omega^{[r]}\theta^{+[r]}}} \left(\sum_{r=I+1}^{n} X^{[r]} - K\right) - \omega^{[i]}\theta^{+[i]}X^{[i]}, \quad \forall i = 1, \cdots, I.
\end{aligned}
$$

Since $\lambda_1^{[i]} > 0$ for $i = 1, \ldots, I$ and $0 \le K^{[i]} \le X^{[i]}$ for $i = I+1, \cdots, n,$ the following conditions hold:

$$K \le \sum_{r=I+1}^{n} X^{[r]},$$

$$
\begin{aligned}
X^{[i]} &< \frac{\frac{1}{\omega^{[i]}\theta^{+[i]}}}{\sum_{r=I+1}^{n} \frac{1}{\omega^{[r]}\theta^{+[r]}}} \left(\sum_{r=I+1}^{n} X^{[r]} - K\right), \forall i = 1, 2, \cdots, I, \\
X^{[i]} &\ge \frac{\frac{1}{\omega^{[i]}\theta^{+[i]}}}{\sum_{r=I+1}^{n} \frac{1}{\omega^{[r]}\theta^{+[r]}}} \left(\sum_{r=I+1}^{n} X^{[r]} - K\right), \forall i = I+1, \cdots, n.
\end{aligned}
$$

Case 3.4: $\lambda_1^{(i)} = 0$ for all $i = 1, \cdots, n,$ and $\lambda_2^{(i)} = 0$ for all $i = 1, \cdots, n.$

Now it only remains to consider the case in which $\lambda_1^{(i)} = 0$ and $\lambda_2^{(i)} = 0$ for all $i = 1, \ldots, n.$ Since there is no divergence in the values of $\lambda_1^{(i)}$ and $\lambda_2^{(i)}$, rearrangement does not make a difference. Nevertheless, we will use the ordered indices $[i]$ here for consistency.

In this case, conditions now become

$$\omega^{[i]}\theta^{+[i]}(K^{[i]} - X^{[i]}) + \mu = 0, \quad \forall i = 1, \ldots, n$$

$$0 \leq K^{[i]} \leq X^{[i]}, \quad \forall i = 1, \ldots, n$$

$$\sum_{i=1}^{n} K^{[i]} = K.$$

Solving this system gives us

$$\begin{aligned} K^{[i]} &= \left(1 - \frac{\frac{1}{\omega^{[i]}\theta^{+[i]}}}{\sum_{r=1}^{n} \frac{1}{\omega^{[r]}\theta^{+[r]}}}\right) X^{[i]} + \frac{\frac{1}{\omega^{[i]}\theta^{+[i]}}}{\sum_{r=1}^{n} \frac{1}{\omega^{[r]}\theta^{+[r]}}} \left(K - \sum_{r \neq i} X^{[r]}\right) \\ &= X^{[i]} + \frac{\frac{1}{\omega^{[i]}\theta^{+[i]}}}{\sum_{r=1}^{n} \frac{1}{\omega^{[r]}\theta^{+[r]}}} \left(K - \sum_{r=1}^{n} X^{[r]}\right), \quad \forall i = 1, \cdots, n. \end{aligned}$$

Since we assume there is a system-wide shortage, $K - \sum_{r=1}^{n} X^{[r]} \leq 0$, and thus we get $K^{[i]} \leq X^{[i]}$ for all $i = 1, \ldots, n$. Then, the only required condition for this result to hold is $0 \leq K^{[i]}$ for all $i = 1, \cdots, n,$ which gives us

$$X^{[i]} \geq \frac{\frac{1}{\omega^{[i]}\theta^{+[i]}}}{\sum_{r=1}^{n} \frac{1}{\omega^{[r]}\theta^{+[r]}}} \left(\sum_{r=1}^{n} X^{[r]} - K\right), \quad \forall i = 1, 2, \cdots, n.$$

This result can actually be seen as a special case of **Case 3.3**, where $I = 0$, and therefore we can combine the results from these two cases.

In summary, the result depends on whether there is a system-wide surplus or shortage. In the event of a system-wide surplus (i.e., $K^{(i)} > X^{(i)}$ for $i = 1, \ldots, n,$), the optimal allocation in each region is given by

$$K^{(i)} = \left(1 - \frac{\frac{1}{\omega^{(i)}\theta^{-(i)}}}{\sum_{r=1}^{n} \frac{1}{\omega^{(r)}\theta^{-(r)}}}\right) X^{(i)} + \frac{\frac{1}{\omega^{(i)}\theta^{-(i)}}}{\sum_{r=1}^{n} \frac{1}{\omega^{(r)}\theta^{-(r)}}} \left(K - \sum_{r \neq i} X^{(r)}\right).$$

In the event of a system-wide shortage (i.e., $0 \leq K^{(i)} \leq X^{(i)}$ for $i = 1, \ldots, n,$), it has been demonstrated that the solution can be found by sorting $\lambda_1^{(i)}$ in such a way that the first

$I = 0, 1, \ldots, n-1$ of them are greater than 0. If I is 0, then all $\lambda_1^{(i)} = 0$. The I here should satisfy the following conditions, $K \leq \sum_{r=I+1}^{n} X^{[r]}$,

$$X^{[i]} < \frac{\frac{1}{\omega^{[i]}\theta+[i]}}{\sum_{r=I+1}^{n} \frac{1}{\omega^{[r]}\theta+[r]}} \left(\sum_{r=I+1}^{n} X^{[r]} - K \right), \forall i = 1, 2, \cdots, I,$$

$$X^{[i]} \geq \frac{\frac{1}{\omega^{[i]}\theta+[i]}}{\sum_{r=I+1}^{n} \frac{1}{\omega^{[r]}\theta+[r]}} \left(\sum_{r=I+1}^{n} X^{[r]} - K \right), \forall i = I+1, \cdots, n,$$

where if $I = 0$, then the first inequality can be discarded. Once I is identified, the optimal allocation in each region is given by $K^{[1]} = \cdots = K^{[I]} = 0$,

$$K^{[i]} = \left(1 - \frac{\frac{1}{\omega^{[i]}\theta+[i]}}{\sum_{r=I+1}^{n} \frac{1}{\omega^{[r]}\theta+[r]}} \right) X^{[i]} + \frac{\frac{1}{\omega^{[i]}\theta+[i]}}{\sum_{r=I+1}^{n} \frac{1}{\omega^{[r]}\theta+[r]}} \left(K - \sum_{r=I+1}^{n} X^{[r]} \right), \quad \forall i = I+1, \cdots, n.$$

Since $\lambda_1^{(i)}$ are sorted, the final result should have been re-sorted accordingly. However, the conditions are the same regardless of the ordering. Finally, we relabel I and $n - I$ for the sake of simplifying the notations in the main text, and hence $X^{(i)}$ should be sorted in descending order instead.

Appendix B: Parameter Values in Numerical Examples

This section offers an inventory of all model parameters used in earlier sections. The same sets of parameters are used for all calculations in the three-pillar framework.

Table 4: Demand assessment parameters; values are chosen in the ranges provided in Tables 2 and 3

Parameter	Value
Percentage of intensive care patients requiring ventilators (class I_3)	0.9
Units of PPE required per exposed patient (class E)	5
Units of PPE required per hospitalized patient (class I_2)	15
Units of PPE required per intensive care patient (class I_3)	20

Table 5: Ventilator planning parameters (Porpora, 2020; Rowland, 2020; Patel, 2020)

Parameter	Value
Participating states	New York, Florida, California
Cost of possession per unit per day (c_j)	1
Initial stockpile cost per unit (c_0)	25,120
Daily production rate (a)	10 units
Shortage/surplus cost (θ_j^+/θ_j^-) in Figure 8a	1,000/1,000
Shortage/surplus cost $(\tilde{\theta_j^+}/\tilde{\theta_j^-})$ in Figure 8b	1,000/20
Time-varying weight (ω_j)	Proportional to daily demand X_j

Table 6: PPE planning parameters

Parameter	Value
Participating states	New York, Florida, California
Cost of possession per 1,000 units per day (c_j)	0.01
Initial stockpile cost per 1,000 units (c_0)	0.5
Daily production rate (a)	50,000 units
Shortage cost (θ^+)	1
Time-varying weight (ω_j)	Proportional to daily demand X_j

Table 7: Ventilator/PPE allocation parameters

Parameter	Value
Participating states	New York, Florida, California
Shortage/surplus cost $(\theta_j^{(i)+}/\theta_j^{(i)-})$	1
Weight for resources allocation in region i at time j ($\omega^{(i)}$)	Proportional to m

Canadian Institute of Actuaries
360 Albert Street, Suite 1740
Ottawa, ON K1R 7X7
613-236-8196
head.office@cia-ica.ca

cia-ica.ca

The Canadian Institute of Actuaries (CIA) is the national, bilingual organization and voice of the actuarial profession in Canada. Our members are dedicated to providing actuarial services and advice of the highest quality. The Institute holds the duty of the profession to the public above the needs of the profession and its members.